



HAL
open science

Science data visualization in planetary and heliospheric contexts with 3DView

Vincent Génot, Laurent Beigbeder, D. Popescu, Nicolas Dufourg, Michel Gangloff, Myriam Bouchemit, S. Caussarieu, Jean-Philippe Toniutti, Joelle Durand, Ronan Modolo, et al.

► To cite this version:

Vincent Génot, Laurent Beigbeder, D. Popescu, Nicolas Dufourg, Michel Gangloff, et al.. Science data visualization in planetary and heliospheric contexts with 3DView. *Planetary and Space Science*, 2018, 150, pp.111-130. 10.1016/j.pss.2017.07.007 . insu-01566291

HAL Id: insu-01566291

<https://insu.hal.science/insu-01566291>

Submitted on 4 Mar 2021

HAL is a multi-disciplinary open access archive for the deposit and dissemination of scientific research documents, whether they are published or not. The documents may come from teaching and research institutions in France or abroad, or from public or private research centers.

L'archive ouverte pluridisciplinaire **HAL**, est destinée au dépôt et à la diffusion de documents scientifiques de niveau recherche, publiés ou non, émanant des établissements d'enseignement et de recherche français ou étrangers, des laboratoires publics ou privés.



Distributed under a Creative Commons Attribution - NoDerivatives 4.0 International License



Science data visualization in planetary and heliospheric contexts with 3DView



V. Génot^{a,*}, L. Beigbeder^b, D. Popescu^b, N. Dufourg^c, M. Gangloff^a, M. Bouchemit^a, S. Caussarieu^b, J.-P. Toniutti^b, J. Durand^c, R. Modolo^d, N. André^a, B. Cecconi^e, C. Jacquey^a, F. Pitout^a, A. Rouillard^a, R. Pinto^a, S. Erard^e, N. Jourdane^a, L. Leclercq^d, S. Hess^f, M. Khodachenko^{g,h}, T. Al-Ubaidi^g, M. Scherf^g, E. Budnik^a

^a IRAP, Université de Toulouse, CNRS, UPS, CNES, Toulouse, France

^b GFI, 1 rond-point du général Eisenhower, 31400, Toulouse, France

^c CNES, 18 av. Edouard Belin, 31400, Toulouse, France

^d LATMOS/IPSL, UVSQ Université Paris Saclay, UPMC University Paris CNRS, Guyancourt, France

^e LESIA, Observatoire de Paris, 5 place Jules Janssen, 92195, Meudon Cedex, France

^f ONERA, Toulouse, France

^g IWF, Graz, Austria

^h SINP-MSU, Moscow, Russia

A B S T R A C T

We present a 3D orbit viewer application capable of displaying science data. 3DView, a web tool designed by the French Plasma Physics Data Center (CDPP) for the planetology and heliophysics community, has extended functionalities to render space physics data (observations and models alike) in their original 3D context. Time series, vectors, dynamic spectra, celestial body maps, magnetic field or flow lines, 2D cuts in simulation cubes, etc. are among the variety of data representation enabled by 3DView. The direct connection to several large databases, the use of VO standards and the possibility to upload user data makes 3DView a versatile tool able to cover a wide range of space physics contexts. The code is open source and the software is regularly used at Masters Degree level or summer school for pedagogical purposes. The present paper describes the general architecture and all major functionalities, and offers several science cases (simulation rendering, mission preparation, etc.) which can be easily replayed by the interested readers. Future developments are finally outlined.

1. Introduction

3DView is an interactive visualization application which specializes in the 3D rendering of trajectories and attitudes of interplanetary probes and bodies in the solar system. It is regularly updated and offers numerous missions as diverse as Rosetta, Mars Express, Cluster, Ulysses, Solar Orbiter, JUICE (in addition to the possibility for the user to upload its own trajectories) as well as all planets and moons together with several thousands of celestial bodies (asteroids and comets). For several years now the development strategy of the tool has been geared toward the scientific community, and it transitioned from a purely orbit viewer toward a science tool which now manages both observations and models. It is therefore aimed at the scientific community during the preparation or operational phases of mission exploitation, to offer an immediate knowledge of the mission context for a better interpretation of scientific data.

3Dview offers the visualization of the trajectory of spacecraft and natural bodies and 3D functions like zoom, lighting of objects, instrument fields of view, and customization of external data (user imported objects). Orbit and attitude are handled through SPICE kernels and related files from ESA or NASA repositories, depending on the mission. It has been developed for several years by the GFI Company in collaboration with CDPP, the licence is owned by CNES (GPLv3) and the code is open source. The source code of 3Dview can be found at <https://gitlab.irap.omp.eu/CDPP/3DVIEW>.

Historically, starting in 2005, the 3DView tool was developed for Rosetta mission to visualize its long and complex trajectory towards the 67/P comet (10 years of cruise, 4 planetary flybys and 2 asteroids flybys, the comet approach and escort phases). Integrated in the SONC (Science Operations and Navigation Center/CNES Toulouse) web server, it basically allowed scientists and operational teams to know where the spacecraft was at any moment on heliocentric views and later the

* Corresponding author.

E-mail address: vincent.genot@irap.omp.eu (V. Génot).

<http://dx.doi.org/10.1016/j.pss.2017.07.007>

Received 6 December 2016; Received in revised form 7 July 2017; Accepted 18 July 2017

Available online 20 July 2017

0032-0633/© 2017 The Authors. Published by Elsevier Ltd. This is an open access article under the CC BY-NC-ND license (<http://creativecommons.org/licenses/by-nc-nd/4.0/>).

orientation manoeuvres during the swing-bys (views centered on planets/objets). Quickly, users requested many additional features as the “Instrument view” function (camera field of view), ground trace, longitude/latitude display, ... Meanwhile, to fulfill the needs of space scientists, a generic CNES 3DView (“multimission” version) was set up covering up to 35 missions (Cluster, Mars-Express, Venus-Express, Cassini, Galileo, Ulysses, Voyager1-2, Stereo, Cluster, ACE, Wind, Geotail, SOHO, Giotto, Themis, ...). Any new feature specifically required by one project (i.e the ground station visualization) is automatically shared to the other. At this stage the tool only dealt with trajectory and attitude information.

In 2009, the generic tool was chosen by the CDPF to extend its capabilities in data analysis and to provide added value to its large database. This evolution was implemented in the frame of the FP7 IMPEX project which covered the year 2011–2015 (see Section 6). In 2015 the new version was fully operational and enabled displaying scientific models (analytical and simulation) together with data plotted along orbits. The IMPEX evolution and the ones that recently followed are jointly managed by CNES and IRAP. It now covers up to 60 missions with 75 probes.

In 2014, a new 3DView Rosetta version helped scientists in the selection of the Philae probe landing site thanks to the accurate and regularly updated comet shape model and planned trajectories display. Just after the landing, it helped the Philae position/orientation reconstruction (3D precise Philae model moving on a Digital Terrain Model function with cameras field of view simulation and shadows). However this “3DView Rosetta” remained a closed access version; the present article focuses on the public version.

The content of the paper is the following: we start by introducing the general architecture of the tool, at the software (Section 2) and orbit management (Section 3) levels, we continue with reviewing the analytical models available (Section 4), then how a scene is set up (Section 5) and how observations and models are accessed by interoperable means (Section 6) and displayed (Section 7). Section 8 explains how to export a scene representation in images and movies. Section 9 demonstrates 3DView capabilities through several science cases in different heliophysics and planetology contexts. We conclude by summarizing 3DView key features, showing how it is used today in science and education, and finally exposing what are the next areas of development for the tool. A list of web references is appended. It centralizes the URLs of most of tools, services, libraries, ... which are discussed in the paper, and in the order they appear.

2. 3DView architecture

The overall architecture of 3DView is depicted in Fig. 1. 3DView is made of two main components: the client, which is the only man/machine interface and is launched by the user (generally from a browser or a desktop icon), and the server which provides web-services for orbits, coordinate transformation and models, and procedures for data update. The client uses web-services to manipulate and plot data. It is developed in Java7 with Swing, JAX-WS, Java3D, JFreechart, JMF, NetCDF and XML and has been tested for Windows, MacOSX and Linux (32 or 64 bits). Although they were initially developed for the client, all web-services may be accessed by external applications. For instance the online coordinate transformation tool TREPS, described in a companion paper (Génot et al., 2018), uses the 3DView web-service for frame transformation.

3DView is a “Java Webstart application”. Java Webstart is a technology which allows launching of applications remotely, using the Java Net Launching Protocol (JNLP). SWING, a GUI widget toolkit for Java, and Java3D, a scene graph based 3D application programming interface for the Java platform are used for the 3D display. Table 1 lists all the components used by 3DView. The choice of Java was settled more than 10 years ago. Java support on the long term has been questioned from time to time but it finally proved to be robust enough as maintenance quality (e.g. bug fixing velocity) improved regularly.

Java2 Standard Edition provides a set of java classes allowing to display lists and graphical objects. It includes the SWING package which allows the display of graphical components like applets, frames and dialog boxes. 3DView was developed with the JDK (Java Developer Kit), but only needs the JRE (Java Runtime Environment). Java3D allows rendering and handling three-dimensional geometric objects: all items (including spacecraft, trajectories, simulation cuts, data and model representations, etc) are 3D objects (handled by the Java3D library) except maps which are cylindrically-projected textures. It is uploaded with Java Webstart when the 3D display is launched, if it was not uploaded upon the previous launch (package size is about 3 Mo). The Java Media Framework enables audio, video and other time-based media to be added to applications and applets built on Java technology. It is used by 3DView to create movies in QuickTime format, by concatenation of series of JPEG images. Java JFreeChart allows the display of several types of 2D graphs: curves, histograms, pie charts, etc. Loader3DS, a Java loader for the 3DS file format, is used to load satellites and asteroids models in the main

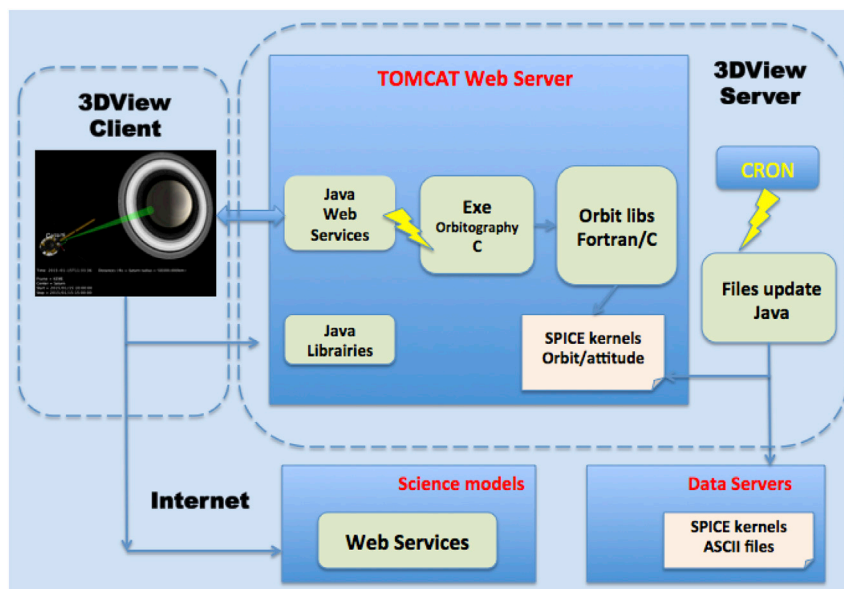


Fig. 1. 3DView overall architecture.

Table 1
JAVA libraries in use in 3DView.

Name	Function
Java2 standard Edition	3DView Client and Server
Java Media Framework	Movie creation from jpeg files
Java3D	Display of 3D objects
JCommon	Package used by JFreeChart
JFreeChart	Display of 2D plots
NetCDF-Java	NetCDF API

view. The NetCDF-Java Library is a Java interface to NetCDF format and many other types of scientific data formats. It was created and maintained by Unidata, and is used by 3DView to read files coming from AMDA (the Automated Multi Datasets Analysis tool of CDDP, see also Section 6).

The 3DView server holds the database of SPICE kernels (see next section) and other associated files necessary to display spacecraft trajectories (satellite models for instance). Texture for planetary surfaces are also on the server side. Science data are stored and maintained externally, and accessed via interoperability means (see Section 6).

3. SPICE kernels for trajectories, attitudes and fields of view

To display the trajectories and attitudes of different bodies, spacecraft or planets, it is necessary to know their positions. This information is given in data files, called SPICE kernels, provided by NASA/NAIF or ESA/PSA, or defined internally by the tool developers (see below). SPICE (Spacecraft Planet Instrument C-matrix Events) which is the U.S Planetary Data System's standard for archiving ancillary data, provides ancillary data related to space missions, that help scientists determine where a spacecraft was located, how a spacecraft and its instruments were pointed, and what was the location, size, shape and orientation of the target body being observed. SPICE is used to organize these ancillary data in collections of stable file types (the kernels). With SPICE, it is possible to compute many kinds of observation geometry parameters at selected times; for example, positions and velocities of planets, satellites, comets, asteroids or spacecraft, size, shape and orientation of planets (planets are ellipsoids whose dimensions come from the SPICE library), satellites, comets, asteroids, orientation of a spacecraft and its various moving structures, instrument field-of-view location on a planet surface or atmosphere. 3DView uses SPICE kernels for all missions (see Fig. 2). They may be directly uploaded from the NAIF, ESA/PSA or other web sites or alternatively generated using NAIF definitions (this is, for example, the case for the Moon Inter-action coordinate System, MIIS, used in section 9.2 for Titan from the definition given in the literature). A direct connection to SSCWeb also allows creating and updating some orbit files related to Earth spacecraft. 3DView developers wrote the code to produce

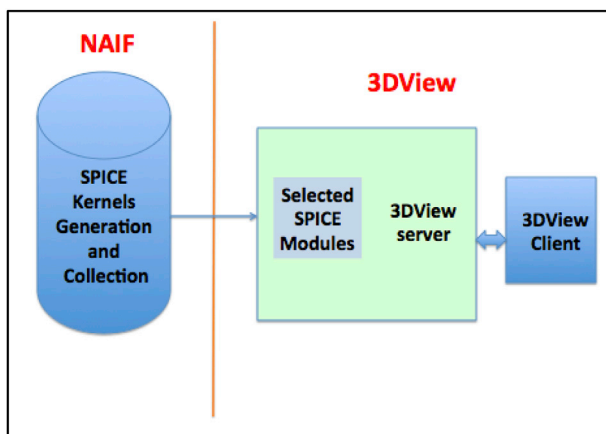


Fig. 2. 3DView link to NAIF.

data (trajectories, attitudes, fields of view) from the kernels by using SPICE libraries.

Users of 3DView can access Instrument Field of View (FOV) and spacecraft attitude from the 3DView server or upload them. Regarding orientation, instruments are simulated in three ways: by a cone, a straight line (java3D objects) or by simulation of the view: positioning of the scene view on the instrument branch: position + viewing angle and angle of view. It is possible to create a view in a separate window. A new view is then created and positioned according to the attitude of the instrument. The target mode of an object leads a placement of the instrument on the main branch of the scene. During the animation, an algorithm calculates its absolute position and moves it.

Spacecraft trajectories may be time shifted relative to their true definition. This can help figuring out how a given region has been mapped by different missions. Spacecraft trajectories whose true orbits are posterior to the scene are displayed in green, whereas the anterior ones are displayed in red.

4. Analytic models for planetary boundaries and magnetic fields

Analytical models for planetary boundary surfaces (bowshock, magnetopause) and magnetic field are available for a variety of bodies including the Sun. These are important representations which enhance the geometrical context into which data (observations or simulations) are analyzed. The boundary models included into 3DView are summarized in Table 2.

Within the tool the bow shock and the magnetopause have editable properties that control their shape and appearance (see Fig. 3). Boundary crossings are marked as colored spheres along the spacecraft trajectories.

At the solar/heliopause scales 3DView also provides models related to the magnetic field: Parker spiral and field lines, and the Heliospheric Current Sheet (HCS). We shall see later that Carrington maps of magnetic data (Section 7.2) and modelled fronts of Coronal Mass Ejections (CME, Section 7.4) may be rendered as well.

The Parker Spiral (Parker, 1958) may be displayed in a 3D scene according to three options (see Fig. 4). By default, a “full” spiral is displayed in the ecliptic plane. The spiral may be extended out of the ecliptic plane; this operation is allowed by an associated control box in which the user can change the number of latitudes (default value is one latitude). The spiral for solar latitude zero is in the ecliptic plane. The solar wind velocity is of course the control parameter for the spiral winding. Alternatively, the user may give the coordinates of a fixed point in the heliosphere by which the field line must pass. This line is associated with a specific control box. Finally the user may select an object (planet or spacecraft) and plot the line passing by this object. The line is displayed in the 3D scene with an associated control box and will be animated when the targeted object moves. Several lines may be plotted simultaneously with the last two options. A “dynamic” capability is provided for several heliospheric spacecraft which have measured or still measure the solar wind velocity. Available spacecraft are those for which solar wind data are provided by the AMDA database (ACE, Wind, ...). A last, still prototype functionality enables the user to upload his/her own field lines from a text file. Close to the Sun the magnetic field lines can really depart from Parker ones and more realistic configuration may be obtained from dedicated modelisation (PFSS, MHD). Modelled lines may also come from more global models like ENLIL or Euhforia.

The Heliospheric Current Sheet (HCS) is the surface where the polarity of the Sun's magnetic field changes orientation. The model by Pei et al. (2012) may be displayed in a 3D scene, associated with a dedicated control box allowing the modification of several parameters, coming from the model itself (tilt angle according to solar cycle, ...) or necessary for the 3D rendering (heliospheric extension, ...), as shown in Fig. 5.

Planetary magnetic fields are generally composed of an internal magnetic field and magnetic disturbance due to magnetospheric currents. Outside the regions containing currents, the internal magnetic field is derived from a scalar potential developed in spherical harmonics using

Table 2
References of analytic models used for planetary boundaries.

Planet	Bow shock	Magnetopause or magnetic pile-up boundary
Mercury	Kallio and Janhunen, 2003 Slavin et al., 2009 Moldovan et al., 2011	Kallio and Janhunen, 2003 Slavin et al., 2009 Moldovan et al., 2011
Venus	Smirnov et al., 1980	none
Earth	Sibeck et al., 1991	Shue et al., 1997
Mars	Trotignon et al., 2006 Edberg et al., 2008	Edberg et al., 2008 Dubinin et al., 2006
Jupiter	Slavin et al., 1985	Slavin et al., 1985
Saturn	Slavin et al., 1985 Masters et al., 2008	Slavin et al., 1985 Kanani et al., 2010

Schmidt vector normalization in conjunction with the Schmidt quasi-normalization of associated Legendre functions. Magnetic field models provide the magnetic field vector in a specific coordinate system. From outputs of models, 3DView transforms the coordinate system and plots the magnetic field lines. 3DView implements two magnetic field models in its server part: T96 for the Earth (Tsyganenko, 1995) and Cain for Mars (Cain et al., 2003). For the Earth, the external field is provided by the Tsyganenko 96 model (see Fig. 6), which includes the solar-wind-controlled magnetopause, region 1 and 2 Birkeland currents, and the interconnection of the magnetospheric and solar wind fields at the boundary. It is controlled by physical parameters: the solar wind pressure, IMF By, IMF Bz and the DST index. The internal field is provided by IGRF. Outputs of the models are used to plot the magnetic field vector or scalar time series, or magnetic field lines for a set of 3D points values on the trajectory of spacecraft displayed on the scene.

In the IMPEx project framework the team at SINP (Moscow, Russia) provided real-time (on the fly) calculation of the magnetic fields of several planets with the paraboloid model approach for the planetary magnetospheres (the PMM models, e.g. Belenkaya et al., 2013 and references therein). SINP team also provides interpolation of pre-calculated 3D-cubes (sets of three-dimensional arrays containing magnetic field vectors, calculated in points of a grid around planets) stored in a database. Both ways use the same PMM approach, which is intended for description of the magnetospheric dynamics, taking into account the intrinsic planetary magnetic field, the magnetopause current magnetic

field, the tail current system magnetic field, the magnetodisc magnetic field, the ring current magnetic field, and the interplanetary magnetic field, penetrated from the solar wind. Such modular structure allows representing the magnetic field inside the magnetospheres of Mercury, Earth, Jupiter, and Saturn. 3DView can display three data products related to the magnetic field of those planets: time series (vector or scalar) along a chosen spacecraft trajectory, 2D cuts from the original 3D cube, and field lines. These products are obtained via dedicated web-services and associated inputs: S/C for time series, slicing plane for the 2D cuts and initiation points for the field lines.

From a 3D scene, it is possible to display 2D rendering for all central bodies: polar view (north and south) and Mercator map are available. The associated context (field lines, footprints, radial projection of spacecraft on the surface) is also displayed and evolves in time and synchronization with the 3D scene as illustrated on Fig. 7.

Additional models for Earth are the Van Allen belts and the South Atlantic Anomaly (SAA) models, generated from the Tsyganenko 96 and AE8/AP8 models respectively.

5. Scene definition and set-up

The 3D graphic scene is the main view of the application. It is part of a 3D window, which is composed of four parts: the menu bar, the animation control, the 3D scene and an information panel. The 3D scene shows selected bodies and all items added from menus like models, instruments views, ground traces or data. Using a mouse or a keyboard, it is easy to navigate through the 3D scene, to rotate the 3D scene around its center, to zoom in and out, to move left or right. The Menu bar provides access to advanced features: preferences, access to models or science data coming from observations or simulations. The animation panel, divided into two parts, gives static information (coordinate system, time range, etc) and real-time display of distances or time shifts. It is possible to control and follow step by step the evolution of the 3D scene through the animation bar. The animation is started with the “Go/Stop” button. The “Step” button allows advancing step by step. The value associated “with frame/s” gives the number of frames per second, which defines the animation speed. The animation may be started from any time included in the time interval chosen for the scene, and restarted automatically and indefinitely with the “Loop animation” button.

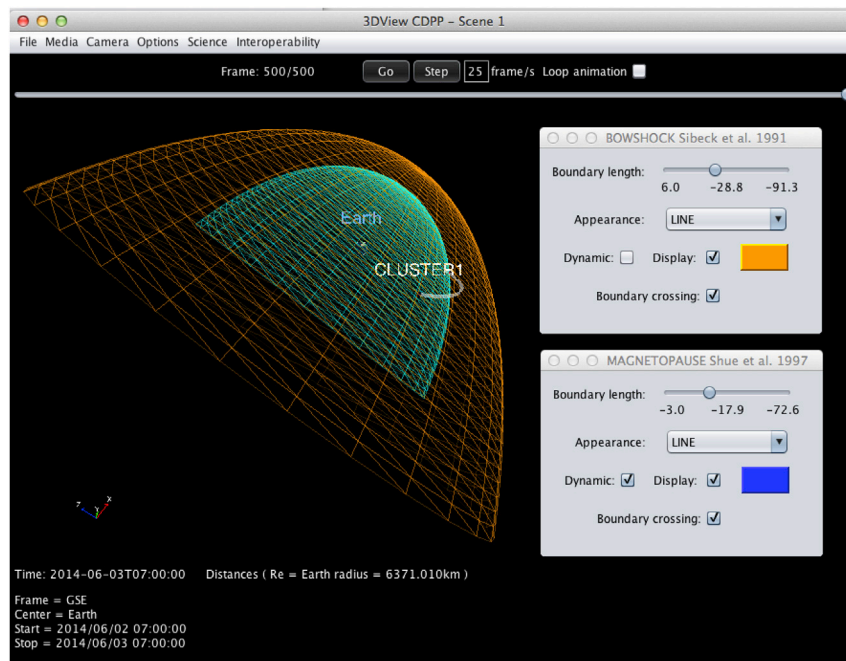


Fig. 3. Bow shock and magnetopause models for the Earth with associated control boxes.

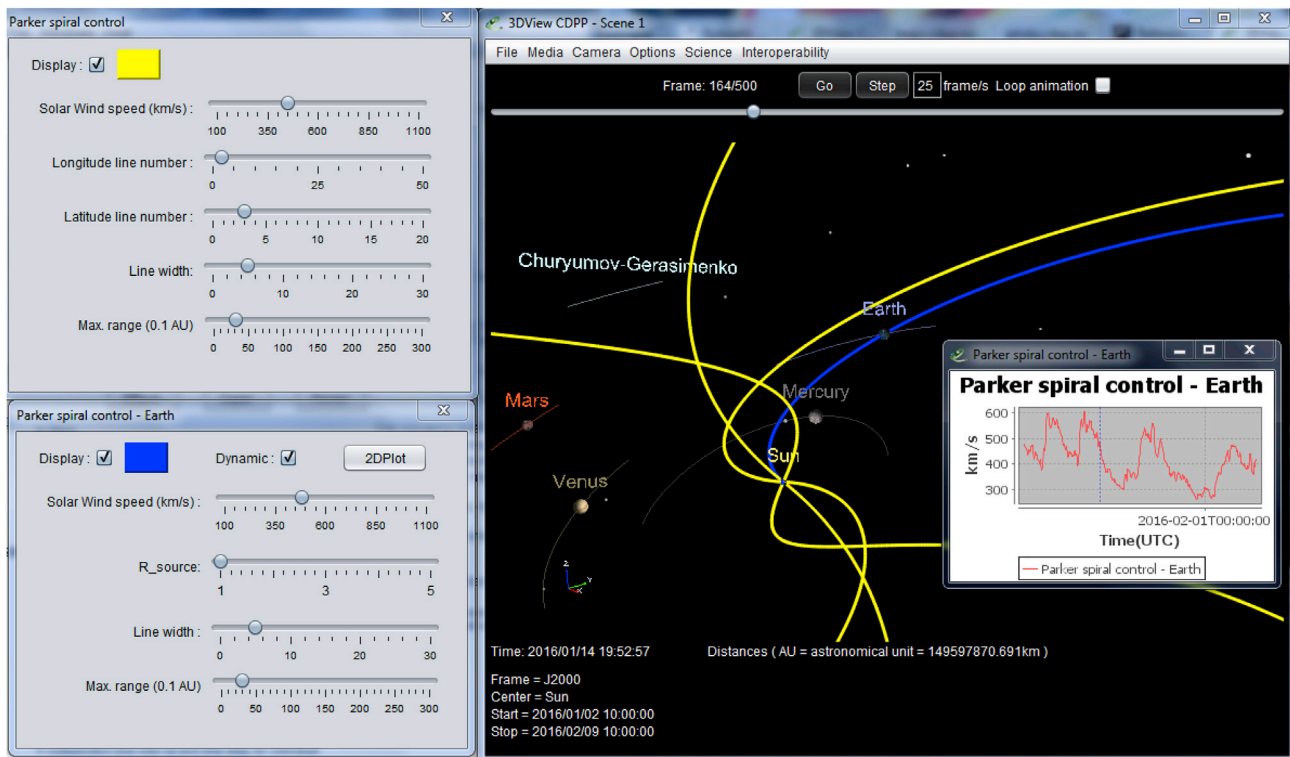


Fig. 4. The Parker spiral in 3D. The 6 yellow lines are for a wind at constant speed (500 km/s). The blue line follows the Earth and takes the velocity measured by ACE as shown in the insert. ACE data are dynamically retrieved from the AMDA database. (For interpretation of the references to colour in this figure legend, the reader is referred to the web version of this article.)

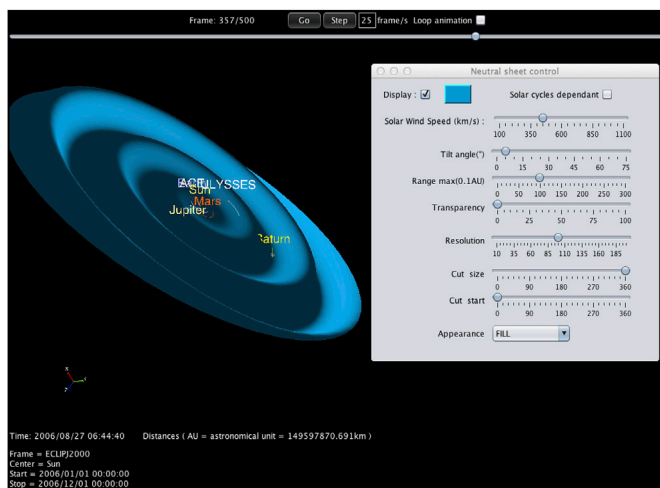


Fig. 5. The Heliospheric Current Sheet (Pei et al., 2012) with its control box.

The scene lighting is managed by two java3d objects: *AmbiantLight* to show the dark parts of objects, and *SpotLight* to simulate the light coming from the Sun. The *SpotLight* object specifies an attenuated light source at a fixed point in space that radiates light in a specified direction from the light source. By default, planets are displayed with their texture and attitude (other texture may be mapped see Section 7.2). The Earth is displayed with its continents, and lighting varying with time. Saturn is displayed with its rings. Several display options are provided in the Options/Preferences menu (see Fig. 8). This menu allows changing the thickness of trajectories, object sizes, number of ticks, displaying or not the name of objects, axes, increase of decrease ambient light.

The main set-up window, through which 3D scenes are created, is the “Manage scene” dialog box (see Fig. 9). It allows the selection of the

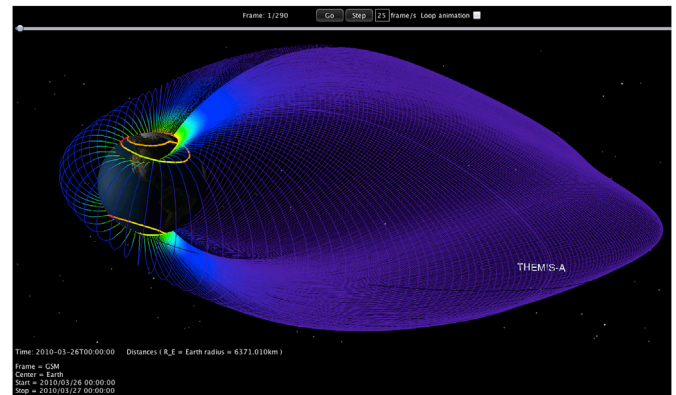


Fig. 6. Magnetic field lines (T96 model) along THEMIS-A trajectory over a day. North and South magnetic footprints are displayed.

3D scene attributes: time interval, coordinate system, time step, center body, spacecraft, natural bodies and time shift. Once created, a 3D scene may be modified at any time. For example, it is possible to add a spacecraft, several natural bodies, or modify the time interval.

Selection of the *Spacecraft* tab displays the list of spacecraft for which orbit and attitude data are available. The *Range* column gives the time span for the corresponding spacecraft; *details* can be obtained on the coverage and time shift can be applied. Selection of the *Natural bodies* tab gives the full list of natural bodies (planets, satellites, main asteroids and comets) divided in two parts: *Preferred available bodies* gives the list of satellites of the body selected as center of the scene and *Other available bodies* gives all the other natural bodies of the solar system registered in 3DView. When a scene has been defined it is possible to search for nearby comets and asteroids (3000 objects from the JPL catalogue). “Nearby” is defined in the tab “Search region” where a sphere centered on a given

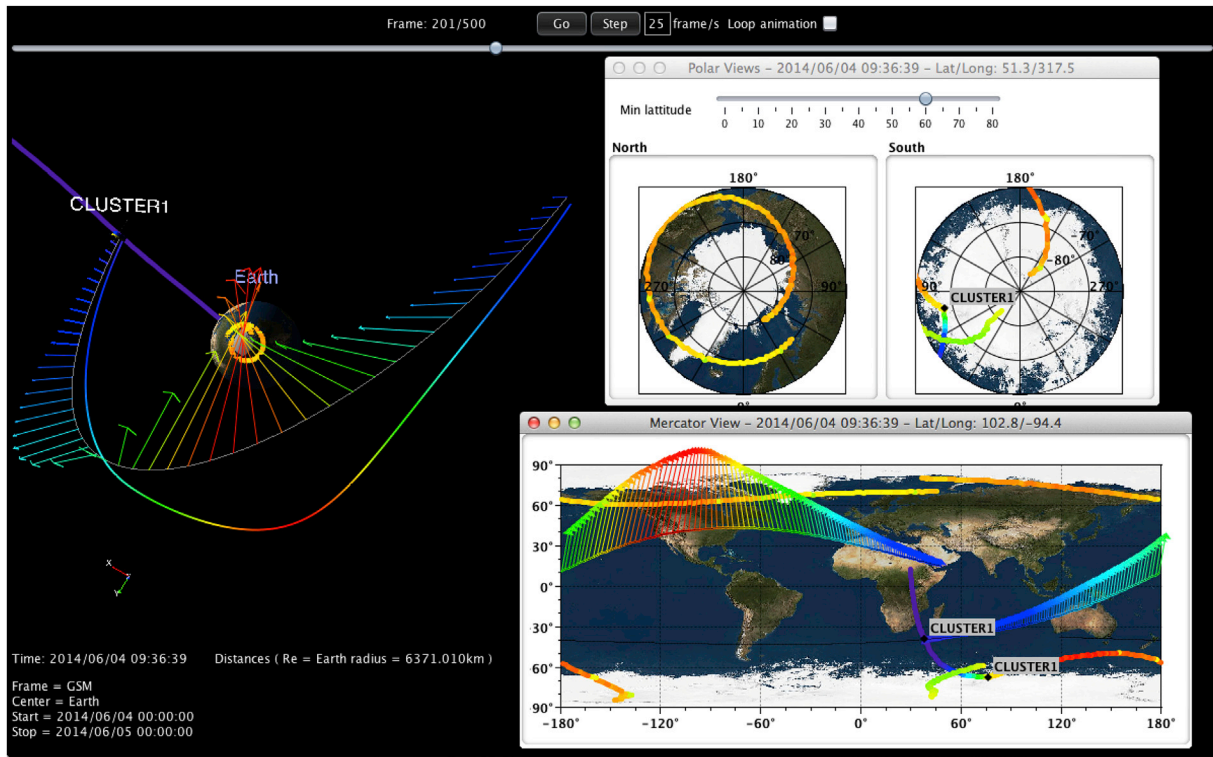


Fig. 7. Magnetic field line (T96 model) passing through Cluster 1, observed magnetic field magnitude (Cluster/FGM) along the trajectory and corresponding polar views and Mercator projection. Footprints and field line projections are seen on these 2D views. Observation data are provided by AMDA web-services.

celestial object is specified with its radius. The list of comets/asteroids within this sphere is displayed and the user can then choose the ones to be added to the scene. The *Coordinate system* menu gives the list of coordinate systems available for the body defined as center in the scene. The *Center* menu gives the list of bodies, which may be selected as center of the scene, with *Sun* as default value. This list contains all the natural bodies for which a coordinate system is available in 3DView (for instance EME2000, or IAU, centered on the body). The *Stars* menu gives several options for the display of stars, with *No star* as default value. Stars are displayed in the 3D scene with a size and luminosity depending on the visual magnitude indicated in the catalogue. The stars are in sub-catalogs taken from the NAIF tycho2 “Master Catalog” (based on data from the ESA Hipparcos mission), with the SPICE starsb software. Catalogs called “all vm” refer to catalogs containing all the stars of visual magnitude less than the indicated number. Catalogs called “corot_vm” contain the stars between the coordinates -15° to 15° of latitude and 89° – 119° and 269° – 299° of longitude. To display areas observable by COROT, with stars of magnitude lower than 10, two catalogs are used: one for longitudes ranging between 89 and 119 and one for those between 269 and 299.

All information displayed in the “Manage scene” window comes from the 3DView server, which provides them through the orbit web-service.

6. Access to remote data

One of the strengths of 3DView is its ability to access scientific data from various suppliers. These data may be derived from observations made by scientific instruments of many missions or from simulations using a variety of models. It is therefore possible to compare, in a single 3DView scene, observed and simulated data interpolated along the trajectory of spacecraft. This is made possible thanks to the presence in 3DView of software layers managing the interface with many data providers of space physics and planetary sciences data. These layers are compliant with standards defined by several international bodies

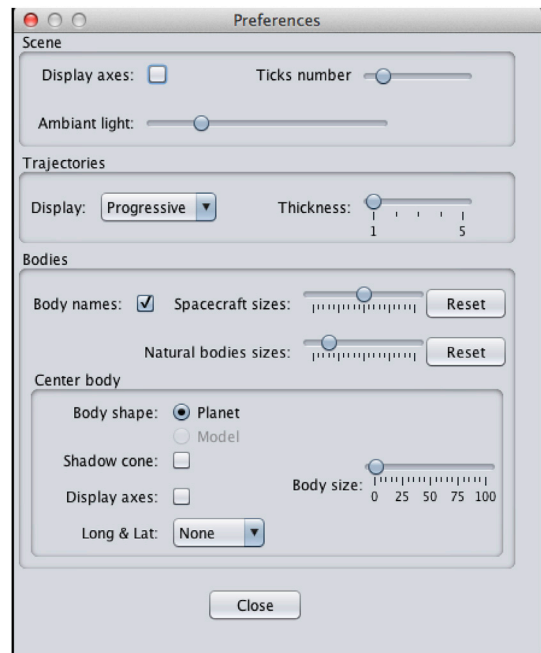


Fig. 8. Preference menu parameterizing the scene and its trajectories and bodies.

ensuring interoperability between data providers and software tools. Such facilities, IMPEX and VESPA, are described in the following paragraphs. Science data may also be accessed from the user's local disk, or using the SAMP protocol.

IMPEX (Integrated Medium for Planetary Exploration, 2011–2015) was a collaborative project of the “Exploitation of space science and exploration data” theme in the frame of the FP7 program of the European

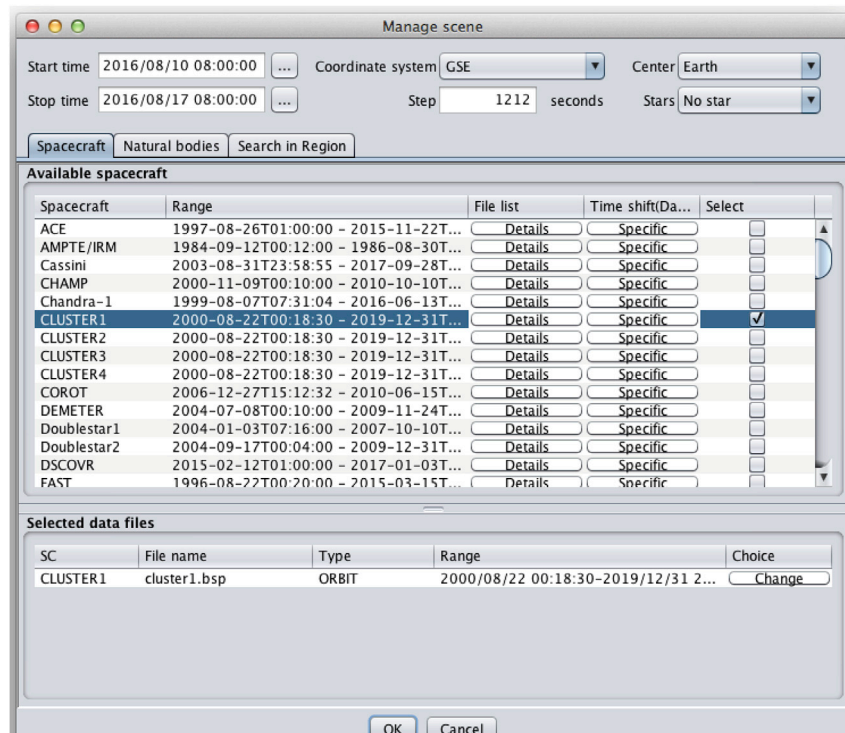


Fig. 9. 3D scene management window where time interval, spacecraft, and natural bodies are specified. Default center and coordinate systems depend on spacecraft selection.

Union. IMPEX aimed at the creation of an interactive framework where data from planetary missions are interconnected with numerical models providing the possibility of simulating planetary phenomena and interpreting space mission measurements, testing models versus experimental data, performing further improvements of models, filling gaps in the measurements by appropriate modelling runs, and performing preparation of specific mission operations. The main pillars of the IMPEX system are the IMPEX Protocol and the IMPEX Data Model which allow for the exchange of data between various nodes as captured in the IMPEX Configuration. Enabling the connection between tools like 3DView and data providers was a challenging task, in particular when complex scientific data were involved. The approach of IMPEX is highly compatible with the vision of the International Virtual Observatory Alliance (IVOA) that calls for astronomical datasets and other resources to work as a seamless whole. The IVOA initiative, as does IMPEX, aims at connecting systems in order to be able to easily exchange science data and leverage functionalities of a rich set of tools. Thus, IMPEX uses several standards that originated out of the VO community that were defined by IVOA. Among them is the VOTable format that is heavily used in IMPEX, to exchange trajectories etc. SAMP (see below) is another IVOA standard that allows desktop applications as well as web-based tools to communicate with each other in a straightforward way (see for instance Génot et al., 2014). The overall architecture of IMPEX is depicted in Fig. 10.

3DView is a key component of the IMPEX infrastructure, giving access to scientific data coming from observations or simulations. During the IMPEX project, the capabilities of 3DView were extended, including the display of time series along the trajectory of spacecraft, 2D cuts in simulation cubes, spectrograms and field lines. From several simulation databases implementing the IMPEX protocol, users may fly “virtual” spacecraft, by calculating model parameters along the trajectory of a given spacecraft. A pop-up window gives access to IMPEX data represented as a tree. Data are classified by Data Provider Name (e.g. LATMOS), Object of the Solar System (e.g. Mars), Simulation Run, Product Type (e.g. Time Series), and physical parameter (e.g. Magnetic field). The tree must be opened to access the different resources. As the tree expands by the addition of new resources this calls for a refined functionality (e.g.

text search) which is under study. A set of filters allows shortening the list of data, according to the scene time range, the center body, or the spacecraft selected in the scene. After selection, data are displayed in the 3D scene. For example, scalar or vector time series are displayed along the trajectory of the previously selected spacecraft. Fig. 11 represents an example of IMPEX data selection.

3DView uses the IMPEX infrastructure to access 3D hybrid models for several planets (from the Finnish Meteorological Institute, FMI, and the Laboratoire Atmosphère, Milieux, Observations Spatiales, LATMOS), MHD models for the Earth magnetosphere (from FMI), 3D Paraboloid Magnetospheric Model for several magnetospheres (from the Skobel'syn Institute of Nuclear Physics, SINP), and observational data from many spacecraft via the AMDA, CLWeb, CDAWeb databases. These three databases hold a wide variety of spacecraft in-situ observations in the ionospheric, magnetospheric, heliospheric and planetology domains. Finally a testbed to access simulation runs from CCMC was added for a few runs.

Other simulation or observation databases are welcome to join the IMPEX infrastructure. They must only implement the IMPEX protocol and their holdings will become accessible through tools like 3DView.

SAMP, the Simple Application Messaging Protocol, is a standard provided by the IVOA, for software tools to exchange control and data information, thus allowing users to treat separately developed applications as an integrated suite. The protocol has been designed within the context of the International Virtual Observatory Alliance (IVOA), but the design is not specific either to the Virtual Observatory (VO) or to Astronomy. It is used in practice for both VO and non-VO work with astronomical tools, and is suitable for non-astronomical purposes as well. SAMP allows software tools to exchange messages. At the core of SAMP is the hub which is a service used to route messages between clients, making application discovery straightforward; the hub is intended to simplify the actions of clients, and each client only needs to locate the hub. SAMP is one of the ways used by 3DView to get data from external databases. 3DView “listens to” the Hub, waiting for time series data to be displayed along the trajectory of spacecraft.

VESPA (Virtual European Solar and Planetary Access) is an

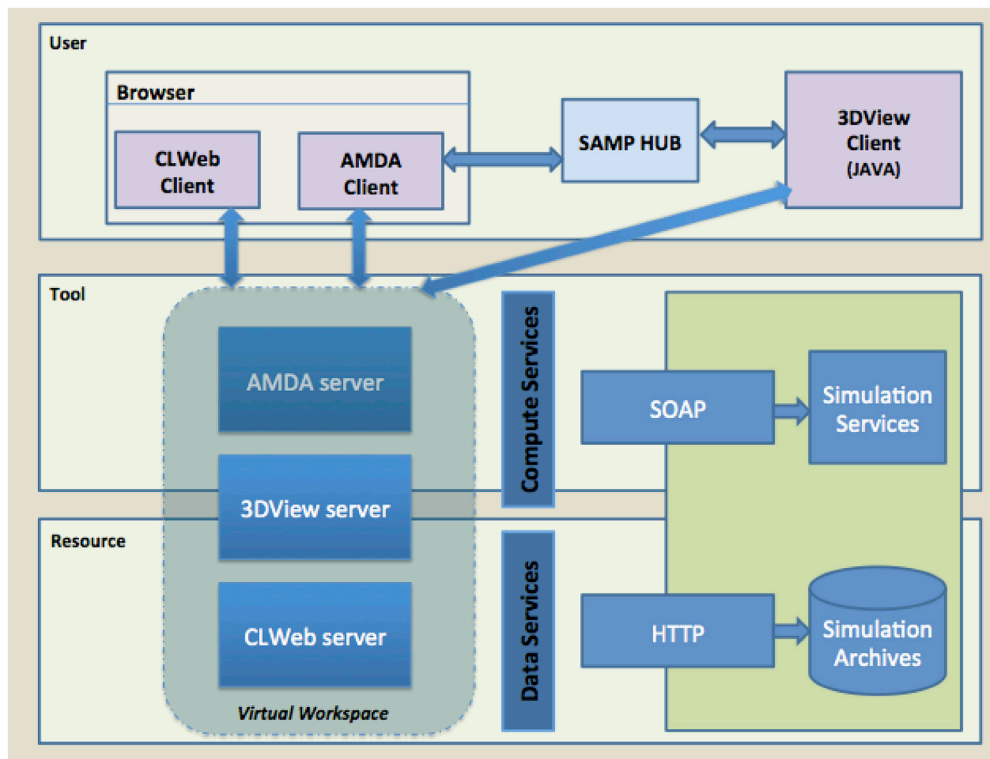


Fig. 10. 3DView in the FP7 IMPEX infrastructure.

infrastructure developed within Europlanet, a project funded by the Horizon 2020 program of the European Union. It started in September 2015 for four years. It is a major step towards the integration of planetary data into the Astronomy Virtual Observatory, thus benefiting from the many years of development in data provision and interoperability in astronomy. The aim of VESPA is to improve data mining and analysis capabilities within and beyond the European planetary sciences community. VESPA provides access to a large pool of data providers covering science disciplines with a broader scope than planetary sciences and including heliophysics, plasmas physics, solid phase spectroscopy, atomic and molecular physics, exoplanets, etc. These services primarily provide data derived from specific analyses, which complement the calibrated, non-interpreted datasets archived by space agencies or ground-based organisations whose main mission is the preservation of original data in the long run. These derived data are provided in standard formats to specialists of other fields (json, VOTable, CDF, JPEG, ...).

VESPA has defined a specific protocol, called EPN-TAP (Erard et al., 2014), to handle the communication between clients and data providers (see also Erard et al., 2018). EPN-TAP is made of two components: the IVOA's Table Access Protocol, used to access data stored in tables, and EPNCore, a metadata model developed to describe planetary sciences data in a standard way. EPNCore inherits several attributes of the PDAP protocol provided by the IPDA, and the SPASE metadata model (PDAP is used to manage the search and exchange of planetary data between space agencies, while SPASE is used by the Heliophysics community). EPNCore is composed of a set of mandatory parameters, common to all fields of planetary sciences, and several optional attributes. Using EPN-TAP, data are accessed in two steps. The first one consists in searching for available EPN-TAP services registered in the IVOA registries, while the second step consists in sending a query searching for data according to specific values of the parameters contained in a table, to filter the database contents. EPN-TAP queries are sent to services simply using HTTP GET or POST. The query is composed of a URL of the service, followed by a specific request expressed with the ADQL language.

A Java library has been designed and developed (by the tool

developing team, in the VESPA context) to manage the low level functions of the protocol. The two main functions of the library are:

- Search the IVOA registry to find relevant services providing data through EPN-TAP
- Send an EPN-TAP query to all these services.

The implementation of VESPA capabilities in 3DView (see Fig. 12) provides users with the access to a large set of planetary sciences data. A search interface allows users to query data services compliant with the EPN-TAP protocol, and to select data based on desired science parameters: a target (planet or natural satellite), a time span, a referenced region on a target and a product type (i.e. spectrogram, image, map, ...). Query results are displayed by 3DView, with an access URL, used to get the actual data (which can be downloaded or SAMPed). The science case 2 details how EPN TAP is used within 3DView.

7. Science data representation

This section explores the multiple ways 3DView can render science data. The data representation can indeed be attached to spacecraft bodies or trajectories, or the central body of the scene, and help exploring 3D simulation cubes or other complex structures.

7.1. Data along spacecraft trajectories

Observations as well as simulations may be accessed from remote data providers as explained in Section 6; these data can be displayed in a 3D scene along the trajectories of spacecraft as time series of vectors or scalars, field lines passing through the spacecraft, or spectrograms. A control box is associated with each quantity. This control box allows the modification of the line width and height for scalar time series, arrow width and length for vector time series, or height for spectrograms. It allows also the modification of the color scale, and gives access, for scalar time series, to a set of statistical analysis functions (Mean, Max, etc). The

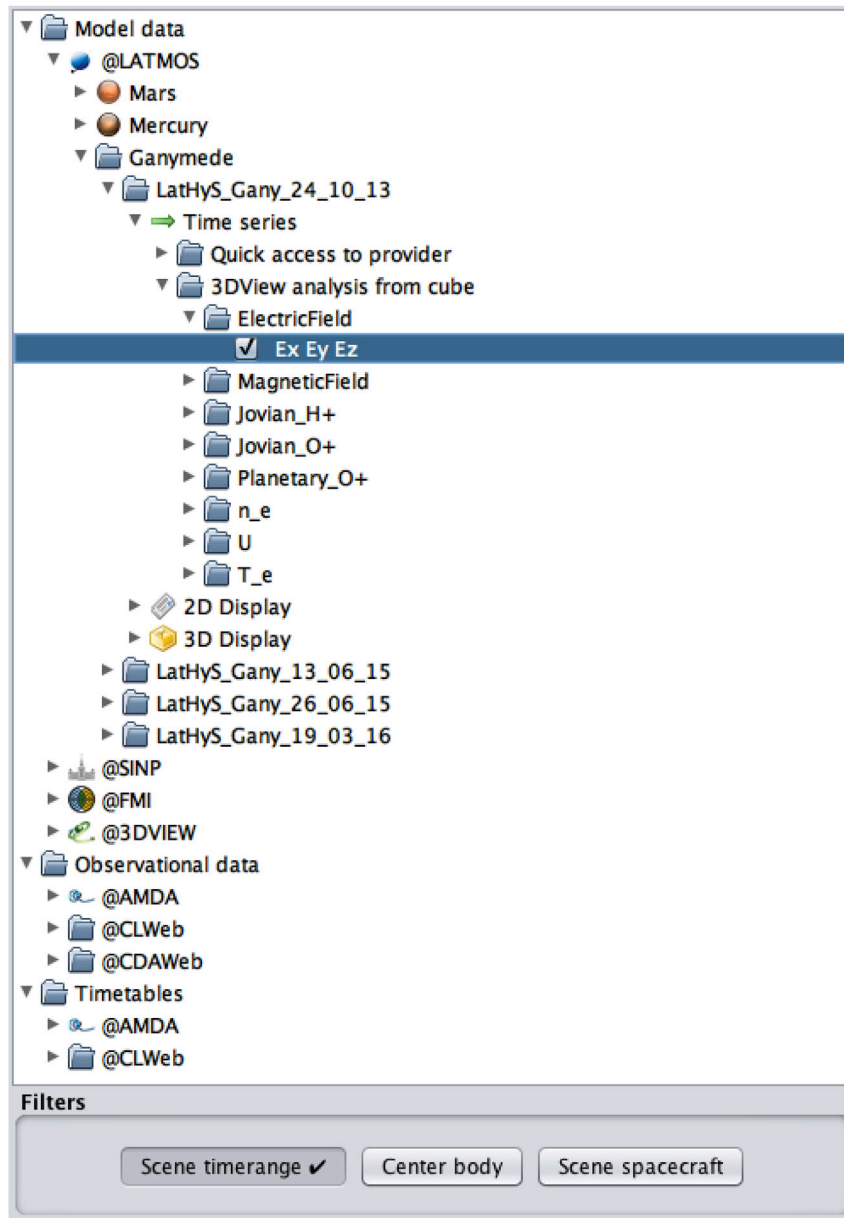


Fig. 11. The data selection window giving access to simulations and observations (from the AMDA, CLWeb, CDAWeb, LATMOS, SINP, FMI databases) and time tables. Data are stored in successive directories down to the parameter level. In this example, the electric field components Ex Ey Ez from a 3D Ganymede simulation at LATMOS is chosen to be plotted as a time series. A panel on the right (not shown) would open to offer the selection of spacecraft (already in the scene) along which trajectories the electric field should be interpolated for display.

3D plot may be accompanied by a classical 2D plot, as illustrated in Fig. 13 which shows a scene with CLUSTER 1 around the Earth and the plot of the magnetic field magnitude from a remote database (AMDA) along its trajectory. In the control box (named “Scalar CLUSTER1 |b|”) several options are provided: show/hide the 3D plot, plot the log of values, change the line width and height, the color scale. Several statistical functions to be applied to the original data on sliding window are offered. Clicking the 2Dplot button opens a new window containing the same plot in 2D. The AVG (average) statistical function is applied to the original data provided by the remote database.

Fig. 13 (right panel) shows the same scene with the magnetic field vector also taken from AMDA. The options are different from those in the previous plot dedicated to scalar time series: *Arrow length or width*, *Sample density* which defines the number of vectors displayed on the S/C trajectory; *Color min* and *Color max*, *Animated*, *Display* and *Log Mode* are the same as those defined for scalar time series.

Depending on the type of data selected, a dedicated “reader” is

executed by 3DView. This reader extracts data from the file and stores them in an array. Afterwards, a new object related to these data is created. This allows plotting the data depending on parameters like color scale. A control box allows the modification of the plot. Time series may be displayed according to a variable sampling. Default is the original sampling of the data. This default value may be increased to reduce the amount of data to be transferred. Sampling may be changed via a special window displayed after the selection of a scalar parameter in the “Remote data (IMPEX)” menu. An illustration of how spectrograms are displayed is shown on Fig. 14: the spectrogram is plotted as a ribbon of adjustable height along the trajectory of the spacecraft.

As described in Section 4 magnetic field lines passing through spacecraft can be displayed for a variety of planetary models, either analytical (T96 and A2000 for the Earth, Cain for Mars, Parker for the Sun, ...) or interpolated in 3D simulations. The server part of 3DView defines the entry points of the service, and the starting points of the field lines may be configured in a dedicated window. Thanks to the IMPEX

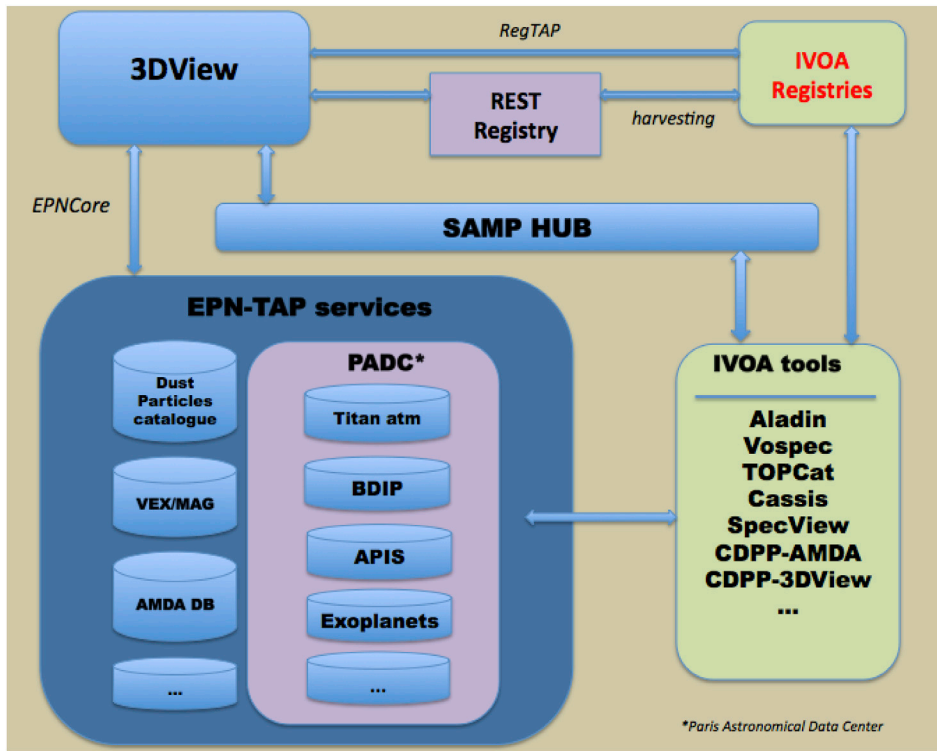


Fig. 12. 3DView in the Europlanet 2020 RI-VESPA infrastructure.

infrastructure, field lines are provided for the Earth, Mars, Venus, Mercury, Saturn and Jupiter.

A functionality for statistical analysis along spacecraft trajectories has been recently added. For any scalar parameter a 3D histogram or a data cube can be constructed from the accumulation of the parameter in a parallelepiped grid on a large enough time span. A standard cube is calculated and 2D cuts are displayed, associated with a control box similar to those for simulation described in Section 7.3. The color of each cell of the cube represents the statistical property (mean, min, max, standard deviation) of the distribution of accumulated physical parameter values along the trajectory of the spacecraft within the cell. The larger the time span the better statistics is acquired as spatial regions will be better sampled. The time resolution of the data considered and the spatial resolution of the grid have to be adjusted to optimize

the rendering.

Although 3DView already offers a wide variety of data, users may want to ingest their own data. The new data may be the orbit and attitude of a new spacecraft (the supported formats for attitude data are quaternion or 3D rotation matrices), the field of view of instruments (by providing cone and direction angle), science data including event lists, maps for planets, satellites or the Sun (Carrington maps). This is explained below.

Time is the very first parameter in many space physics studies, consisting in analysis and characterization of events. Time tables or event lists are therefore important elements to be processed and exchanged by scientists. Each event of a Time Table is characterized by a start time, an end time and a series of optional parameters. Created by scientists from statistical or data mining studies, they are provided to the community via

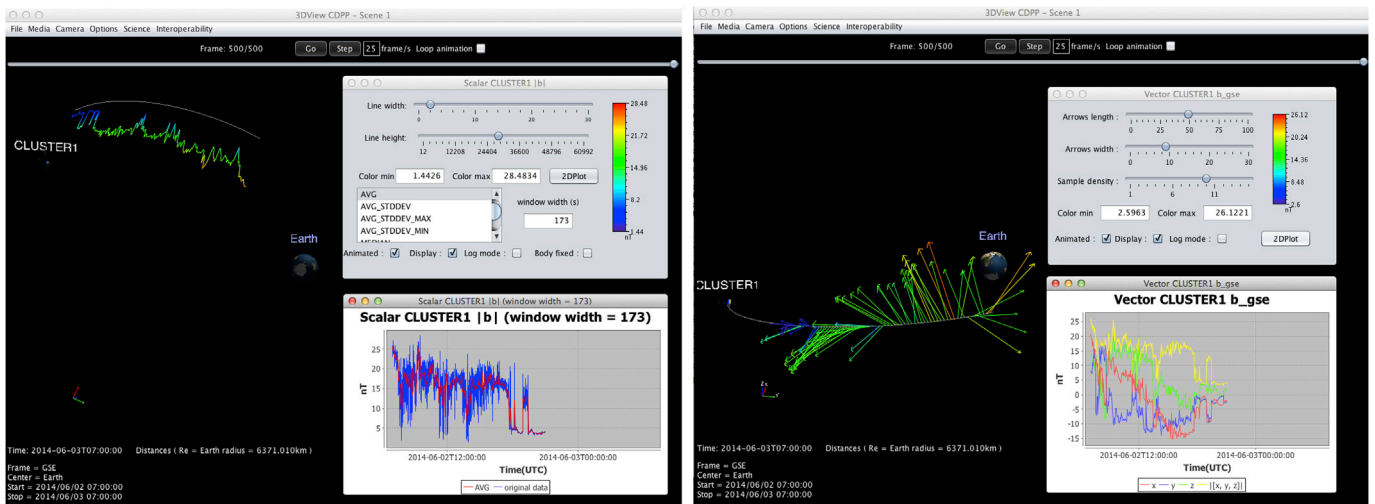


Fig. 13. Cluster 1 magnetic field along its trajectory (magnitude on the left, vector on the right).

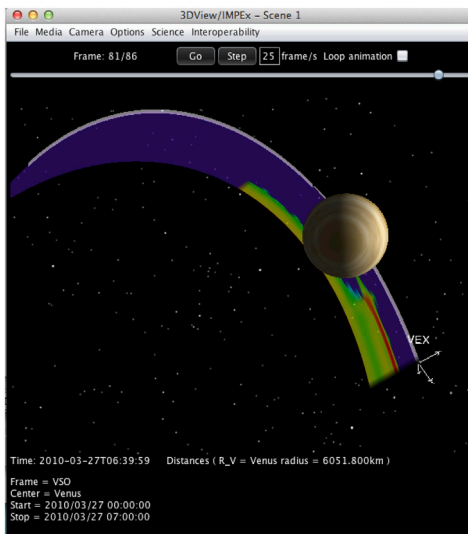


Fig. 14. Spectrogram observed by ASPERA4 onboard Venus Express. The height of the ribbon is adjustable to optimize the scene.

dedicated project web pages, via tools (in AMDA, the Propagation Tool, ...) and are more and more frequently available as numerical extra material in publications (for instance the Co-rotating Interaction Region list in Plotnikov et al., 2016, or the Flux Transfer Event list in Karimabadi et al., 2009). They may come from search tools based on orbit or conjunction criteria, on mathematical criteria applied on the content of databases (see AMDA), or on machine learning algorithms. 3DView allows the creation of Time Tables from a scene as well as the visualization of Time Tables coming from remote servers. The creation of Time Tables in 3DView is available from the animation bar. After positioning the animation cursor at START and STOP times, the user clicks on the Add Time button to save the corresponding time period. At the end of this iterative process, clicking on the *Generate Time Table* button saves the set of time intervals on the local hard disk. Time Tables are displayed along object trajectories (see Fig. 15). Every portion of the trajectory corresponding to a time interval belonging to the Time Table is highlighted/colored.

Time Tables can be directly uploaded in 3DView by the user or acquired via web-service from external tools like AMDA or CLWeb.

A description of instrument field of view (FOV) and spacecraft attitude provides important capabilities regarding mission planning, data contextualization and comparison to models. Scientists may access these parameters directly in 3DView, or upload them. A dedicated GUI allows importing custom orientation data. SPICE Kernels for instrument FOV (IK, FK) and Attitude Kernels (CK) are used for all missions providing them on the NAIF server ... FOV visualization is provided in a dedicated window. Fig. 16 gives an example for instruments of the JUNO mission.

Finally, users may add a spacecraft to the scene, by giving a spacecraft name, a coordinate system and the name of a file containing orbit data, located on the local disk. The format of this orbit file may be ASCII or VOTable. Once the spacecraft is added to the 3D scene, science data may be plotted on its trajectory. Another option is to upload the trajectory of a spacecraft orbiting the Earth from a file in NORAD “two-line element” set format, or TLE.

7.2. Maps

Central bodies in the 3D scene are displayed with a default map. The default map for the Earth shows its surface, with oceans and continents. Users may insert new maps on or above the central body. Maps may come from a set provided by the server of 3DView, and, as soon as simple longitude/latitude format is followed, they may be uploaded from the local disk or a remote URL. Tuning of transparency is provided through a

dedicated control box. Fig. 17 shows a high resolution map loaded onto Enceladus surface.

Carrington maps of the solar magnetic field may be added on the Sun (see Fig. 18). Datasets from GONG, SOHO, SDO, STEREO-A and STEREO-B are available in 3DView similarly to those available from the companion CDPP Propagation Tool (see also the companion papers by Rouillard et al. 2017, André et al. (2017), <http://propagationtool.cdpp.eu/>). The data used by both tools are listed at http://storms-tools.irap.omp.eu/PropagationTool/CDPP_PropagationTool_fichiers/listing.html. Once this option is activated the related images are mapped onto the solar surface and displayed according to their corresponding times (updates in the scene depends on respective time resolution).

Further extension of 3DView mapping functionalities should be available in the coming months. First, in the frame of Europlanet 2020 RI, a direct connection to the APIS database (Auroral Planetary Imagery and Spectroscopy, Lamy et al., 2015) will allow to display HST images of auroral emissions at giant planets (this is made possible via EPN-TAP, see Section 6). APIS holds FITS files which retain all information on geometry and enable a correct data projection. Other databases will be investigated during the course of the project. Second, in the frame of a CNES contract, an enhancement of ionospheric data representations will target ground based assets like radars and magnetometers to be displayed along side footprints in Mercator or polar maps (see Section 4 and Conclusion).

7.3. Simulation handling

Simulation data can be accessed via the IMPEX infrastructure as explained in Section 6. Flying a virtual spacecraft in a simulation cube and interpolating a given quantity along the orbits ends up with a time series which may be displayed like any observational time series; as such all functionalities described in Section 7.1 are therefore also available for simulated quantities. However exploring 3D cubes can also be done more globally by 1/plane cuts in the 3 dimensions, and 2/following field or flow lines from given starting points. These functionalities are available in 3DView in corresponding interfaces and associated control boxes as

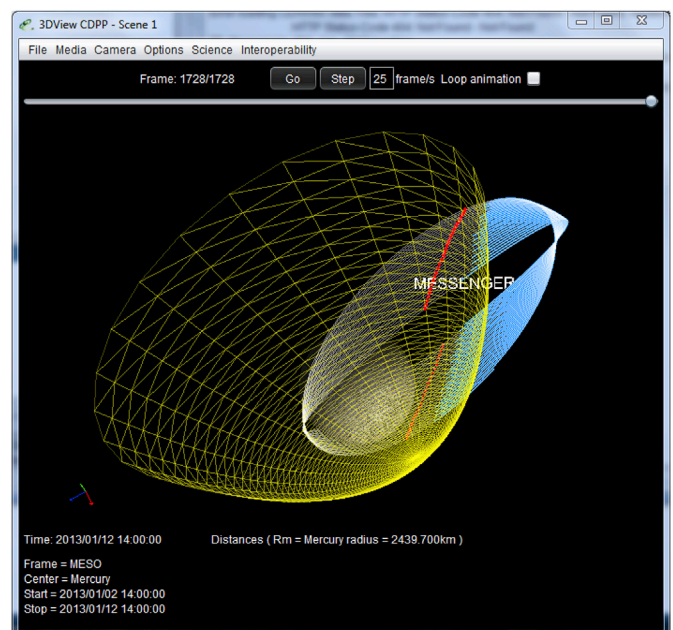


Fig. 15. Solar wind intervals observed by MESSENGER and displayed in blue along its orbit (10 days are shown). The bow shock is illustrated as a yellow surface. The intersections of MESSENGER trajectory and the bow shock are displayed as little red dots. The solar wind time table was produced by the AMDA data mining tool as explained in Section 9.1 concerning the Mercury science case. (For interpretation of the references to colour in this figure legend, the reader is referred to the web version of this article.)

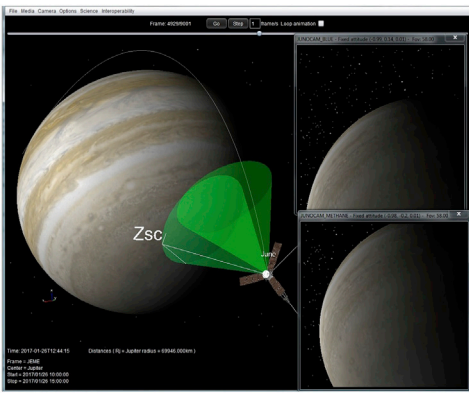


Fig. 16. Fields of view for two apertures of the JUNOCAM instrument on board JUNO.

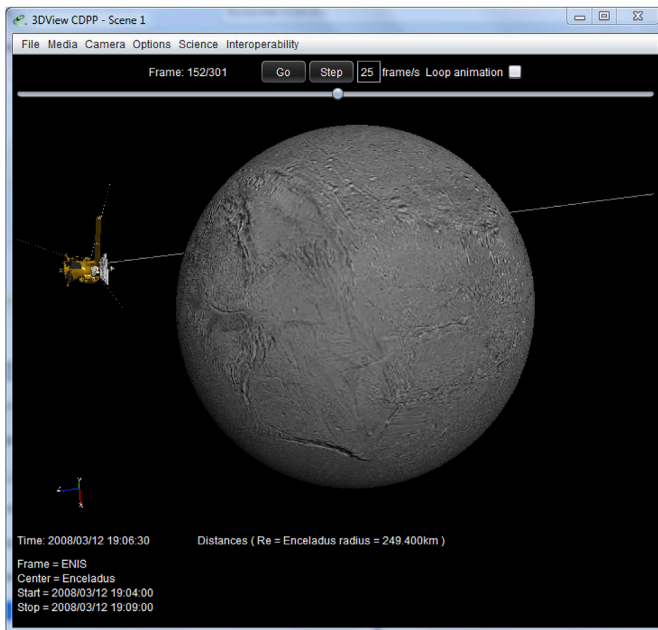


Fig. 17. Enceladus flyby by Cassini (March, 2008). 3DView has a default surface (usually a light image) for all bodies but this illustration shows a high spatial resolution surface map loaded from <http://photojournal.jpl.nasa.gov/> (“Load map” menu in the Science section).

this is briefly illustrated in Fig. 24 for the science case in Section 9.4.1. On the specific aspect of manipulation of complex simulations with 3DView the interested reader is referred to the paper by Modolo et al. which exposes comparison with MAVEN and Mars Express observations.

7.4. Catalogues of coronal mass ejections (CME)

Display of CME fronts is a recent addition to 3DView which makes use of the catalogues produced in the frame of the HELCATS project with the STEREO spacecraft. HELCATS is an EU FP7 project aiming at improving forecasts of solar storms, including their arrival times and impacts on Earth and other planets. As for maps (Section 7.2) these catalogues are also shared with the Propagation Tool (Rouillard et al., 2017). For this functionality, CMEs are modelled as spherical cones following the fixed point approach (Rouillard et al., 2008); initiation time at the Sun, (constant) velocity and direction in HEEQ coordinates are sufficient to uniquely define the CME fronts. In Fig. 19 blue/red colors correspond to CME seen by STEREO A/B respectively.

This functionality is a particular case of catalogue exploitation and could be extended to a wealth of other applications. 3DView is indeed

well suited to display ‘events’ as 3D structures when those can be analytically modelled (see also Time Table rendering, Section 7.1 and Fig. 15).

This functionality has been used to provide supplementary material for a paper (Witasse et al., 2017) which studies the evolution of a CME in the heliosphere in 2014 as it has been observed by a number of spacecraft. More information can be found in the [Supplementary Material Section](#) at the end of the present paper.

8. Save the content of a scene

Several possibilities are provided to users for the backup of the work done in a 3D scene: full backup of scenes, export of data in ASCII or VOTable, backup of orbit and trajectory of objects in a scene. The entire contents of a 3D scene (orbit data, time series science data as well as cubes or cuts) may be saved in a zipped file on the local disk and loaded again later by 3DView. 3DView makes the creation of images or movies from a scene very easy. Images are generated with an off-screen canvas3D, which is attached to a buffer, allowing image creation with several different qualities. A *High Quality* image is three times bigger than the on-screen canvas. For a 800×600 window, the resolution is 2400×1800 pixels. The image generated by the canvas is saved on the local disk in a PNG file. Movies may be generated in two steps: backup of images in JPEG format, and creation with the JMF API of the QuickTime movie from the flux of JPEG images. Orbit data may be saved in a file on the local hard disk. The format of this file may be ASCII or VOTable.

9. Science cases

The text below provides examples on how 3DView may be used in heliophysics and planetology contexts, combining different data sources, models and visualization functionalities (see also the “[Supplementary Material](#)” Section at the end of the paper).

9.1. Science case 1: observations and hybrid simulations compared at Mercury

This science case aims to demonstrate the ability of VO tools to combine successfully observations and global simulation results in order to easily and quickly determine information on the different plasma regions encountered by a spacecraft. We focus on the hermean environment explored by the MESSENGER mission [Solomon et al., 2007]. We attempt to determine the location of the Bow Shock crossings and when MESSENGER spacecraft is magnetically connected to the planet, and eventually to determine if the spacecraft was magnetically connected to reconnected field lines. In this science case we will use two VO-tools, AMDA and 3DView as well as MESSENGER (from NASA/PDS and available in AMDA) data and the Latmos Hybrid Simulation database (Modolo et al., 2018). Information concerning the Hermean simulations are detailed in Richer et al. (2012).

We start the procedure from the LatHyS catalog and we select one of the different simulations of the Hermean environment (e.g. the simulation with the resourceID LatHyS_Merc_15_07_14) either displayed in the LatHyS webpage or in the AMDA workspace explorer. Parsing the simulation tree and the different simulated data products available, the user has access to the simulation input information, such as the solar wind density and speed, moments for several ion species, and the Interplanetary Magnetic Field direction ($\vec{B} = [-18.2, 10.5, 0]$ nT). A constant IMF corresponds to average conditions for that particular case (hybrid codes are demanding models and varying inputs result in large size outputs. The archived simulations are either typical condition examples or particular use cases). Both quantities (observations and simulations) are expressed in the Mercury Solar Orbital coordinate system: X-axis points from Mercury to the Sun, the Y-axis is antiparallel to Mercury’s orbital velocity and Z-axis completes the right-handed coordinate system. The next step is to identify time periods when MESSENGER

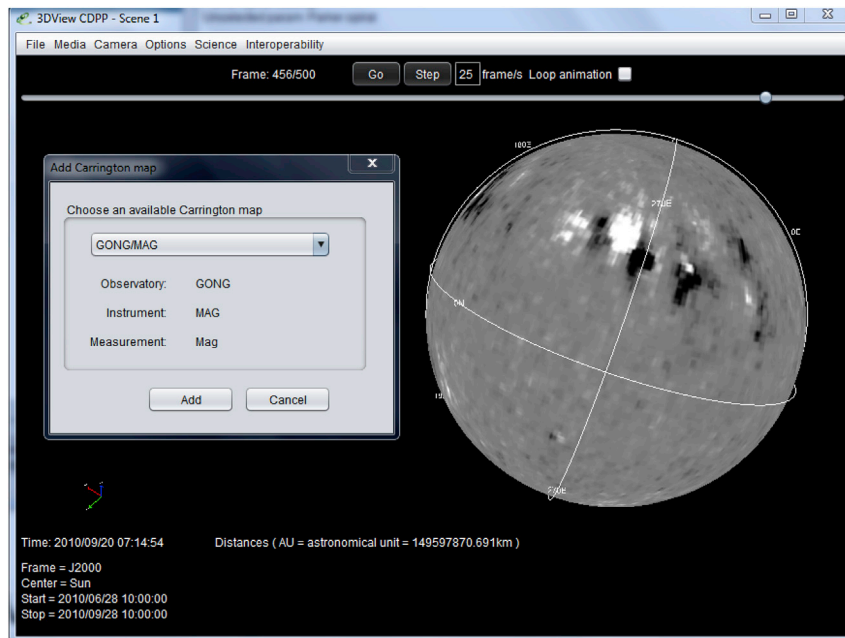


Fig. 18. Magnetic (Carrington) data from GONG/MAG mapped onto the solar surface. Maps are updated as time evolves (and depending on the map temporal resolution).

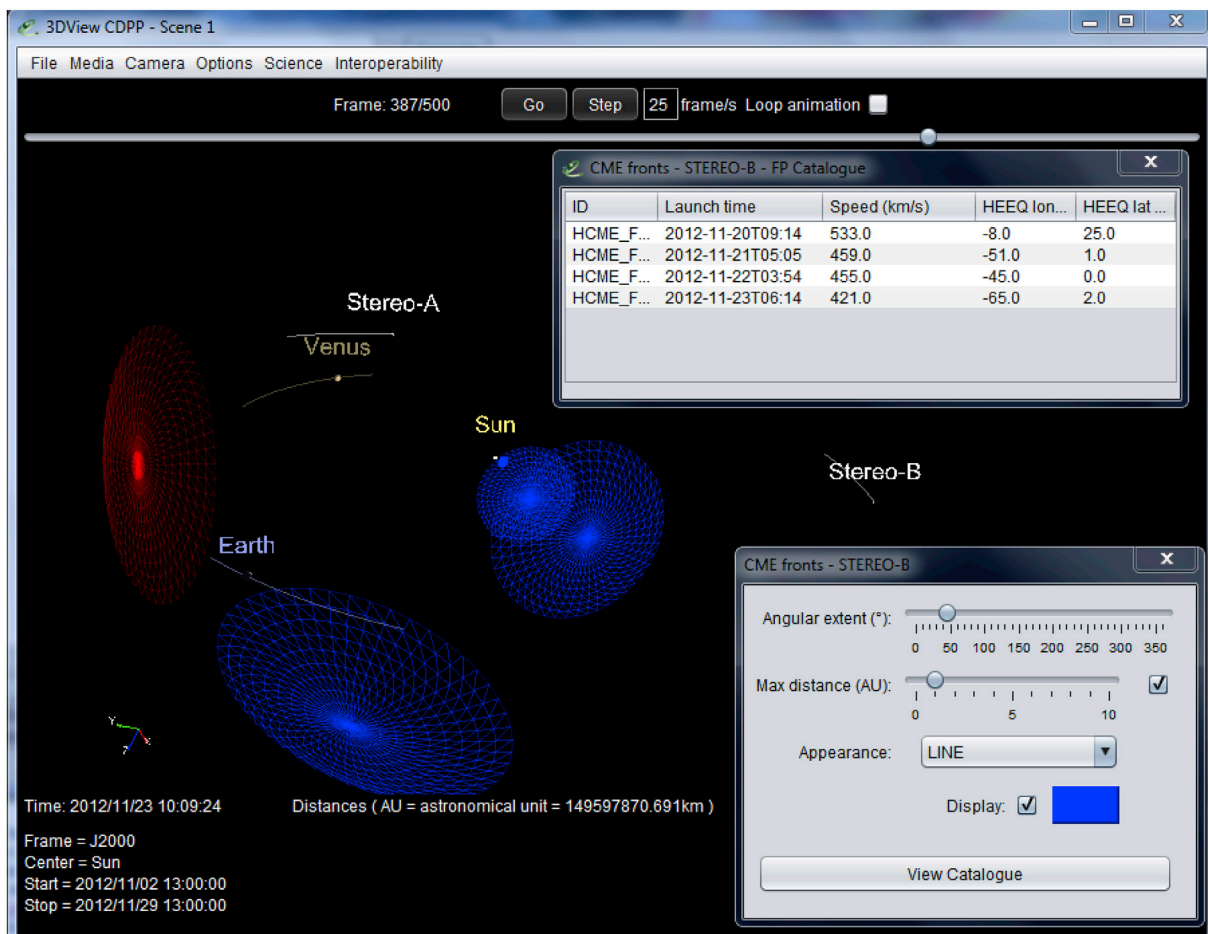


Fig. 19. CME fronts expanding in the heliosphere (fixed point approach). Velocity and direction for each front are obtained from a HELCATS catalogue (which is also shared in the Propagation Tool). The characteristics of the fronts visible in the scene are shown in a dedicated window (upper right in the Figure).

observed similar solar wind parameters (in this case only the IMF orientation since information concerning the solar wind density and speed are not yet available). We use the AMDA data mining facility to determine these time periods. The selection criteria are:

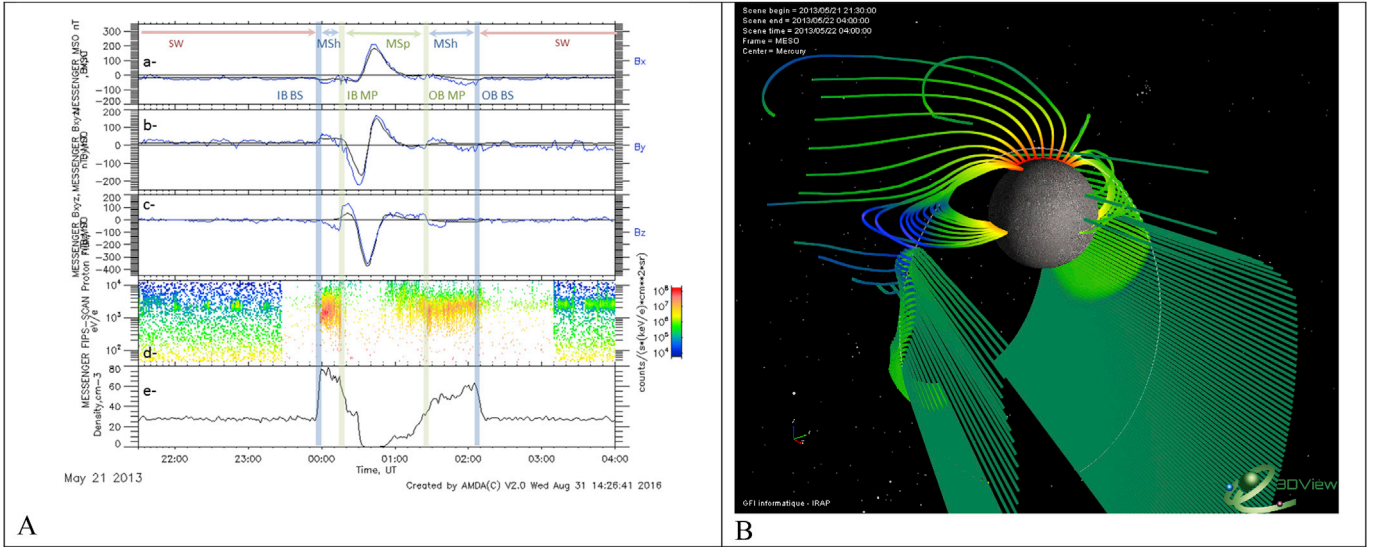


Fig. 20. A- Comparison of MESSENGER observations and simulation results from 2013-05-21T21:30:00 to 2015-05-22T04:00:00 UTC. Panels a to c present the observed (in blue) and simulated (in black) magnetic field components. Panels d and e display the MESSENGER FIPS differential intensity spectra and the simulated electron number density. B- Three-dimensional scene of the MESSENGER orbit with simulated magnetic field lines passing through the spacecraft track. The color code of the field lines indicates the magnetic field intensity varying logarithmically from 1 to 825 nT. (For interpretation of the references to colour in this figure legend, the reader is referred to the web version of this article.)

$$\langle d \rangle_{3000s} > 0.5R_M \quad (1)$$

and

$$\begin{aligned} &(-20nT < \langle B_x \rangle_{3000s} < -16nT) \cup (8nT < \langle B_y \rangle_{3000s} < 13nT) \cup \\ &(-3nT < \langle B_z \rangle_{3000s} < 3nT) \end{aligned} \quad (2)$$

With $\langle d \rangle_{3000s}$ corresponds to MESSENGER distance to the Bow Shock averaged over 3000s, with d defined as

$$d = \sqrt{(X - X_0)^2 + \rho^2} - \frac{p\varepsilon}{1 + \varepsilon \cos\theta} \quad (3)$$

Where X and $\rho^2 = Y^2 + Z^2$ are the MESSENGER position in MSO, X_0 , p and ε are conic parameters used to characterize the average Bow Shock position, respectively the focus point, the focus parameter and the eccentricity. We use the conic parameters determined by Winslow et al., (2013), i.e. $X_0 = 0.5$, $p = 2.75$ and $\varepsilon = 1.04$. $\langle B_i \rangle_{3000s, i=X,Y,Z}$ is the magnetic field seen by MESSENGER averaged over 3000s. The data mining, performed on the time period 2013-01-01 to 2015-04-30, returns a Time Table with about 16 intervals matching the criteria. There is the possibility to manipulate the Time Table, to extend and to shift all intervals by several minutes (here we extended time interval by 180 min) in order to have not only time intervals when MESSENGER is in the Solar wind but full MESSENGER orbits. Obviously it is possible to reverse these steps and start with an observed IMF and identify the best matching simulation in the LatHyS catalog.

For each interval of the Time Table, we can compare the MESSENGER magnetic field data (Anderson et al., 2007) with the simulation results, thanks to the AMDA plotting functionality. Simulation results, corresponding to the selected resourceID, are computed on-the-fly along the MESSENGER track for each interval of the Time Table. It is possible to combine different observed and simulated data sets. Fig. 20-A provides such an example for an event starting on 2013-05-21. The observed magnetic field components (in blue) are compared to the simulated magnetic field (in black) in panels a to c. Particle information is provided by the FIPS instrument (Andrews et al., 2007). FIPS differential intensity spectra and simulated electron number density are presented in panel d and e respectively. A reasonable agreement is found between observations and simulations and we can identify the different regions and

boundaries encountered by the spacecraft. MESSENGER is first located in the solar wind (SW) region identified by a relatively steady IMF and a narrow beam distribution at about 2 keV observed in FIPS spectra. The inbound Bow Shock crossing (IB BS) is identified at about 23:57:00 UTC by a sudden change in the Bx and By components (observed and simulated), a sharp change in the FIPS spectra and a large increase of solar wind density in the simulation. The inbound magnetopause (IB MP) is found at about 00:16:30 UTC and it coincides with a drastic change in the Bz component, the disappearance of magnetosheath (MSH) solar wind ions in FIPS spectra and a rapid decrease of solar wind density in the simulation. The magnetosphere (MSP) is explored by the spacecraft where the planetary magnetic field dominates. The outbound magnetopause (OB MP) and bow shock crossing (OB BS) occurred at about 01:20:00–01:25:00 UTC and 02:11:00 UTC respectively with signatures similar to the inbound crossings. The simulation fairly reproduces the observations and we can use these results in 3DView to explore the three-dimensional characteristics of the hermean environment.

An example of the numerous 3DView functionalities is presented in Fig. 20-B. 3DView provides not only a pseudo-three dimensional and interactive visualization of MESSENGER ephemeris but it also able to display observations and simulation data products in the scene. As an example we can compare the FIPS and simulation ion spectra along the spacecraft track, load 2D plane cuts of simulated fields or ion species quantities, load field or solar wind velocity vectors etc. Fig. 20-B displays simulated magnetic field lines connected to the spacecraft track. In this scene the MESSENGER trajectory is displayed in the MSO coordinate system with a temporal resolution of 120s in order to minimize the restitution of field lines computations. By browsing step by step field lines passing through the spacecraft orbit, we can determine when the spacecraft is magnetically connected to the planet and the location of the footprints on the surface. We found that the spacecraft is located on field lines with at least one end connected to the planet between 00:16:00 UTC and 01:22:00 UTC, which correspond to time interval when the spacecraft is in the magnetosphere. In addition, between 00:30:00 UTC and 00:34:00 UTC the spacecraft might be located on planetary field lines reconnected to the IMF. Such magnetic configurations favored precipitations of charged particles and might have important consequences on the weathering of the surface of the planet.

9.2. Science case 2: T117 Cassini fly-by and data discovery with EPN-TAP

This science case presents how 3DView can be used to display the 3D context of one Titan fly-by by Cassini and how it helps to discover broader planetology data. In Feb, 16 2016 Cassini flew by Titan for the 117th time (T117) with closest approach at about 1000 km (at 23:49:51 UTC). The 3DView scene is set up by choosing Titan as the center body during the interval 2016-02-16 21:00 to 2017-02-17 03:00. The reference frame is Titan Interaction System (TIIS in 3DView) for which the z axis is aligned with Titan's rotational axis, the y axis points from Saturn to Titan, and the x axis completes the system and represents the ideal magnetospheric flow direction. Note that similar frames are defined for other moons DIIS for Dione, ENIS for Enceladus, etc. These frames were specifically coded by the tool developers. Once the scene has been built it is possible to get the 3D perspective of the flyby by, for instance, displaying the approach phase with the altitude profile or look at instrument FOV (which are opened in a separate windows as in Fig. 16). At the time of the paper preparation there is no Cassini data available on databases directly connected to 3DView for this time period; this does not preclude external data to be uploaded by the user.

The last step concerns the ability of 3DView to discover planetology data worldwide from the initial context of the scene (Fig. 21). This is done via the VESPA interface available in the Science menu. To date, as explained in Section 6, the VESPA infrastructure enables us to search for data in 33 different planetology and heliophysics services compliant with EPN-TAP (see also Erard et al., submitted). In the corresponding interface (menu: *Remote data (VESPA)*) the left part of the window contains the list of services, and the right one the detailed response of the selected service. Each line corresponds to a data file and contains several parameters identifying the corresponding data, with an access URL, used to get the actual data, and a thumbnail, when available. Searching for data of interest in the VESPA framework is made directly by 3DView, the context of the scene being pre-selected in the search pop-up window, and compliant data services being directly queried. For the present science case, when the interface is opened Titan is already selected as the Target and the time interval corresponds to the one of the scene. There is an optional possibility to restrict the search to a sub-region of Titan surface by the “Select region” button; this opens a Mercator projection map, the user can define the subset via the mouse and the subsequent EPN-TAP request will be done with these extra parameters. Once the “Search” button is hit the VESPA registry is consulted and services with corresponding data returns corresponding files. For the short time interval of the scene the search returns no data. By extending the time frame (for instance changing the start year to 2006) will provide answer from the “titan” service of PADC/LESIA; this database displays vertical profiles of temperature and composition in Titan's atmosphere obtained by Cassini/CIRS from remote sensing techniques. Thumbnails of the available profiles are displayed in the interface. To access the data themselves, as they cannot be displayed in 3DView “as is”, it is necessary to send them to an external tool, either by downloading them first, or by directly sending them via SAMP to the companion tool (both possibilities are offered by right clicking on the chosen file). For instance in the present case TOP-CAT (Taylor, 2005) can easily plot such profiles. Similarly the EPN-TAP interface shows that (1023) results exist in the APIS database which stores PDF and FITS observations of Titan atmosphere; the FITS files may be sent to Aladin for visualization.

This use case has shown how to easily get the 3D perspective of a particular planetary configuration, and moreover how current interoperability infrastructure enables to extend the richness of data without an a priori knowledge of the user.

9.3. Science case 3: Cluster and Double Star observations of dayside magnetopause

This science case of coordinated observations of Earth's magnetopause by Double Star 1 (Liu et al., 2005) and Cluster (Escoubet et al.,

2001) is based on the work by Pitout et al. (2008). We revisit the event to show what could have been done with 3DView and we shall present what is planned to get a fully integrated conjunction finder and 3D visualization tool.

On 25 February 2004, Double Star 1 and Cluster were both in the southern hemisphere, near the magnetic noon meridian. In their paper, Pitout and colleagues studied the occurrence of flux transfer events and their time evolution as they were observed at both spacecraft. To show their data, the authors had no choice but displaying data as a function of time and position making it sometimes tricky to know what was observed where and when. If 3DView was available at the time, the authors would have displayed their data in a more convenient way by following the time evolution of their data set step by step by displacing the time cursor.

On a static image like the one shown in Fig. 22, one can spot the Flux Transfer Events (FTE) referred to and discussed in the paper as event 2 and 2' (green arrows), and event 3 and 3' (light magenta arrows). They are seen as a sudden and short-lived increase of the magnetic field (here the GSM Bz component) at 03:12 UT and 03:19 UT respectively at Double Star 1 and Cluster. It has to be noted that the individual components of the B-field measured by FGM (Balogh et al., 2001) are not directly available in 3DView. A parameter has to be created in AMDA and called from 3DView: Science → Remote data (IMPEX) → Observational data → @AMDA → private. Then, by making the time evolves in 3DView, it is very easy to spot those FTEs and see the correspondences between the two satellites: the FTEs pop up in Double Star data first and a little later at Cluster.

Furthermore, what has not been done in the paper is the study of the ground signatures of the FTEs. With the current version of 3DView, the search for the ground traces of the satellites and the ground instruments in the vicinity would have been straightforward. Fig. 23 shows a screenshot of the 2D polar plot window of 3DView: northern hemisphere (left) and the southern hemisphere (right) in geographic coordinates. The panel of the right-hand side displays the radial projection on the southern polar region of Cluster (top label) and Cluster and Double Star 1 magnetic projections (reddish traces).

A future version of 3DView (now in development) will comprise enhanced 2D visualization capabilities with the fields of view of ground-based instruments (SuperDARN radars for instance, see Chisham et al., 2007) and the possibilities of displaying their data; and a conjunction search tool (CST) that will allow the user to spot conjunctions between satellites or between satellites and ground-based instruments. The case presented here was found by visual inspection of Double Star 1 and Cluster projected orbits, it would have been found much more rapidly with a CST.

9.4. Science case 4: mission preparation

An interesting aspect of 3DView is to help visualizing and conceiving novel configurations of spacecraft and celestial bodies, in particular thanks to models and simulations. This comes in support to mission preparation which is quickly explored below in planetary and heliophysics contexts.

9.4.1. Ganymede observed by Galileo and compared with simulations in the perspective of JUICE

Preparing a new mission in the light of data from a former mission may be common for Earth orbiting spacecraft but less so for planetology ones. The jovian moon Ganymede has been visited (during short fly-bys only) a few times by the Galileo spacecraft twenty years ago and will only be visited again in about less than twenty years, this time by an orbiter, JUICE (Grasset et al., 2013). 3DView can help aggregating the plasma information collected on this remote body and simulated in the perspective of JUICE (see Fig. 24). The scene is set up with Galileo centered on Ganymede during the closest fly-by for 1h (G2: 1996-09-06); by default the GPHIO coordinate system is chosen (the z-axis is parallel to Jupiter's spin axis, the x-axis is in the direction of the incident flow, and

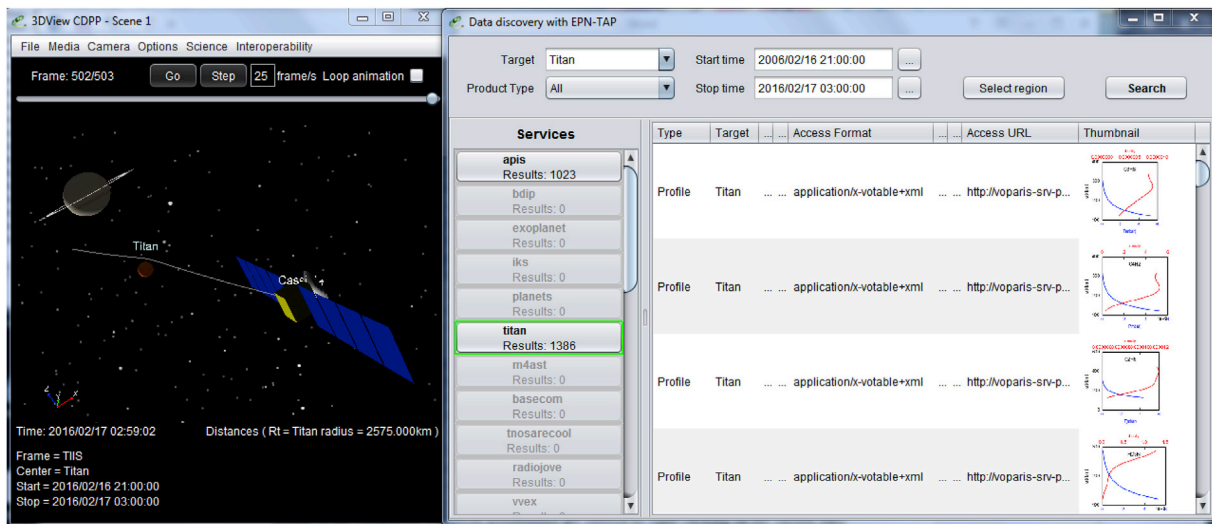


Fig. 21. T117 flyby of Titan by Cassini (left), and (right) the contextual data discovery with EPN-TAP. The target is automatically set to Titan and, for an extended time range, the VESPA services which hold Titan related data are seen in the ‘Services’ column. The ‘titan’ service for atmospheric profiles shows 1386 results, 4 of which are displayed as thumbnail. This profile can then be downloaded or sent to companion tools for analysis. One can see that the APIS database also holds 1023 results corresponding to an HST campaign on Titan in 2009.

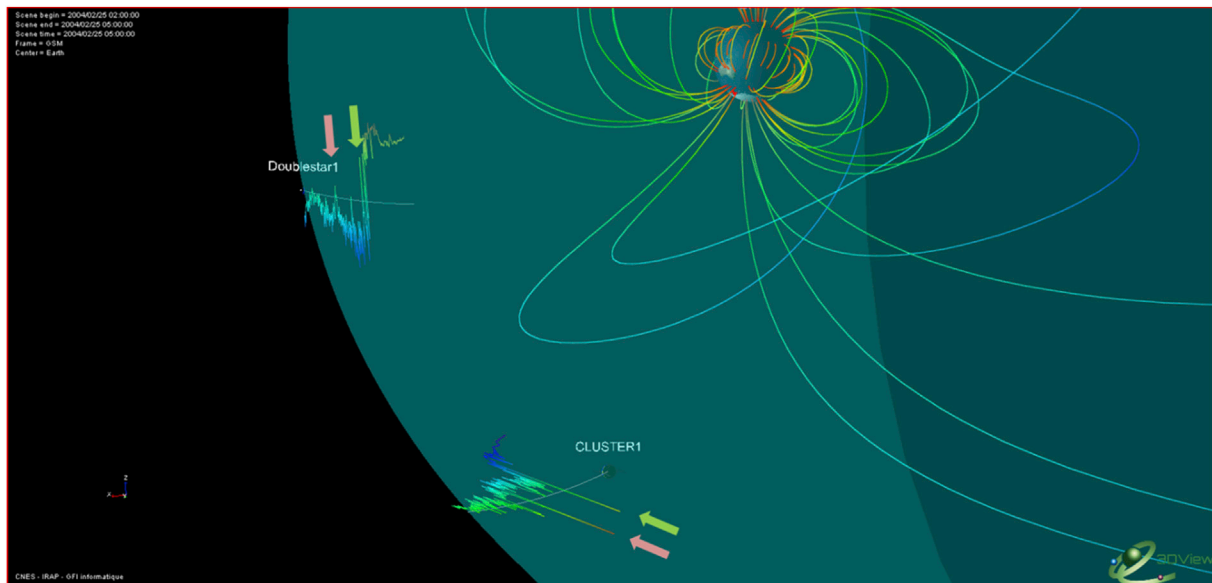


Fig. 22. Magnetic field lines (from T96) and the magnetopause (green area) for the prevailing IMF and solar wind conditions on 25 February 2004 around 03:00 UT. The figure also displays the trajectory of Double Star 1 and Cluster 1 between 02:00 and 04:30 UT and, on top of them, the z-component (in GSM) of the magnetic field measured by FGM aboard both missions. (For interpretation of the references to colour in this figure legend, the reader is referred to the web version of this article.)

the y-axis completes the triad and is mainly directed towards Jupiter). Next we use the time shift functionality to display JUICE orbit 36.5 years later. ‘Future’ orbits are displayed in green, past ones in red. Then we open the ‘Remote data (IMPEX)’ menu to access Galileo data in the Ganymede environment from the AMDA database (the original public data come from the Planetary Data System). The magnetic field amplitude is plotted along the Galileo trajectory. These data are then compared to one recent hybrid simulation (2016-03-19) with the LatHyS code (for instance Leclercq et al., 2016a,b; Modolo et al., 2016, 2017). This simulation was especially designed to be compared with the G1 and G2 flybys. The simulation cube is then explored by different means. First the amplitude of the simulated magnetic field (interpolated along Galileo trajectory) is compared to the observed one and show remarkable agreement. Similarly the simulated magnetic field vector is plotted along JUICE trajectory as arrows in the 3D scene but also as a simple time series plot. More globally a cut in the magnetic field amplitude 3D cube in

performed in the GPHIO XZ plane. 3D cubes can be investigated in several ways: downloading the whole cube on the user disk may take time but more slicing options are then available subsequently; a lighter approach may be to only download pre-calculated 2D slices. This depends on how the modeller database is constructed but both approaches are possible within the IMPEX framework and handled in 3DView. The 2D cut shows a shape corresponding to the magnetic bending of Ganymede magnetic field in the Jovian plasma flow. Only the magnetic field was chosen here for conciseness (and not to overload the Figure) but other data can of course be explored similarly.

Recently, and similarly, the JUICE Science Working Team used 3DView to explore 3D hybrid simulations at Ganymede with the aim to characterize the 13 future fly-bys of the Galilean moon by the ESA mission (times for closest approaches, magnetopause crossings, magnetotail current sheet crossings, ...).

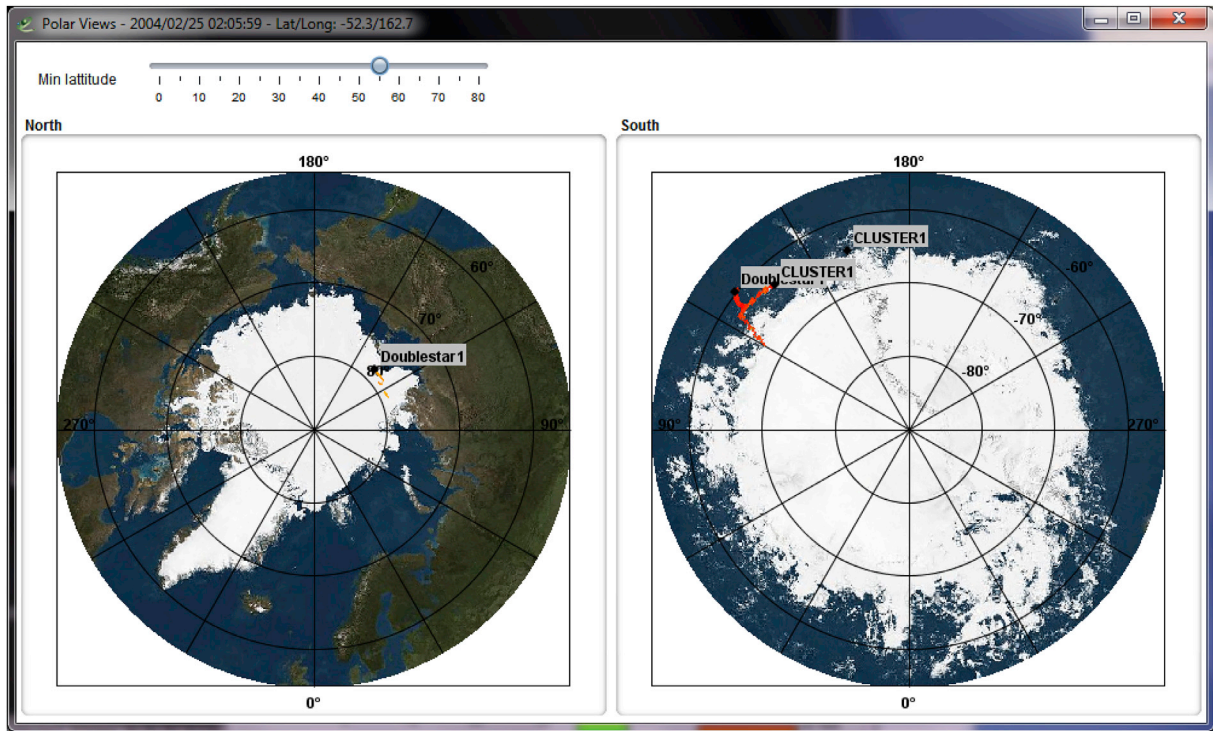


Fig. 23. Polar views of the northern (left) and southern (right) hemispheres. Radial and B-field traces of Cluster 1 and Double Star 1 are displayed.

9.4.2. Solar magnetic connectivity for Solar Orbiter and Solar Probe Plus

For missions like the two next heliospheric missions, ESA/Solar Orbiter (ESA report, 2011) and NASA/Solar Probe Plus (recently renamed Parker Solar Probe), which will combine in-situ measurements and remote sensing, a key issue will be to assess the magnetic connectivity of the probes with the Sun. This will enable to make a direct correspondence between in-situ plasma observations and their potential

origins at the Sun. In the scene below, a configuration of both probes in 2020 is presented. 3Dview enables to display solar magnetic field lines going through the probes for a given solar velocity as illustrated on Fig. 25. However Parker field lines give only a first order of the magnetic field configuration. The interested user can go further by uploading his own field lines coming from models or simulations which may give a better representation of the field close to the Sun in particular. An

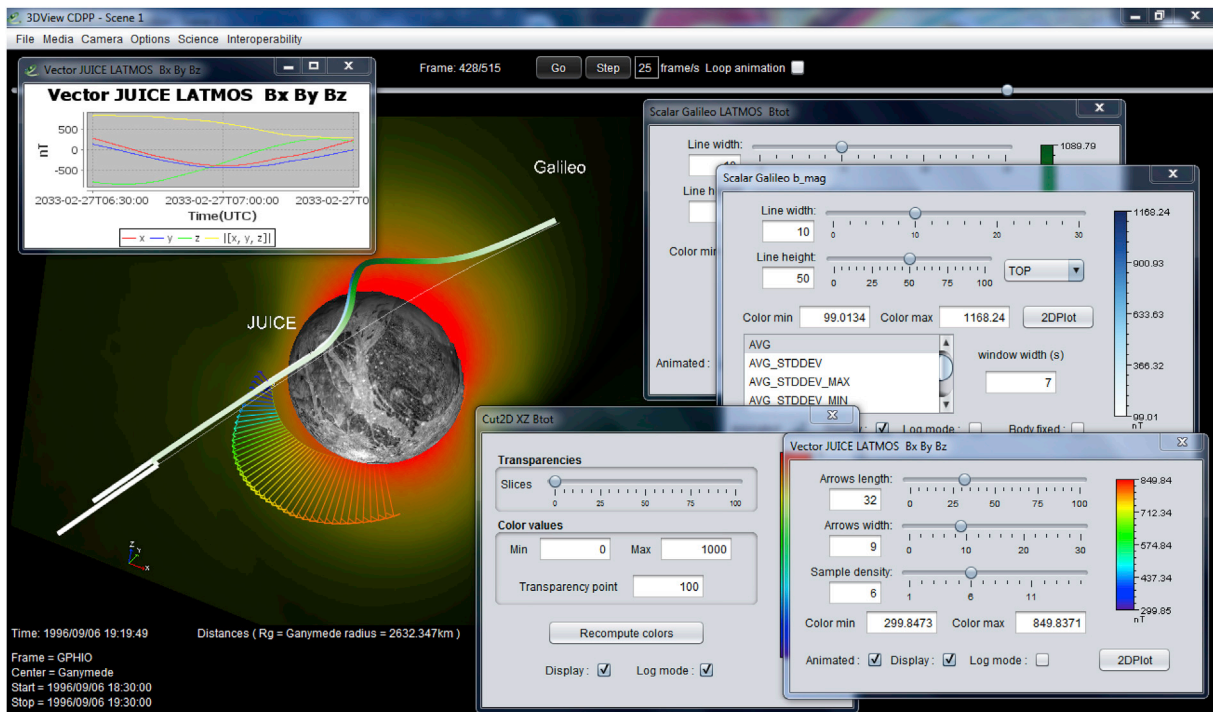


Fig. 24. Observed (Galileo) and simulated (JUICE) data in the Ganymede environment (see text for details).

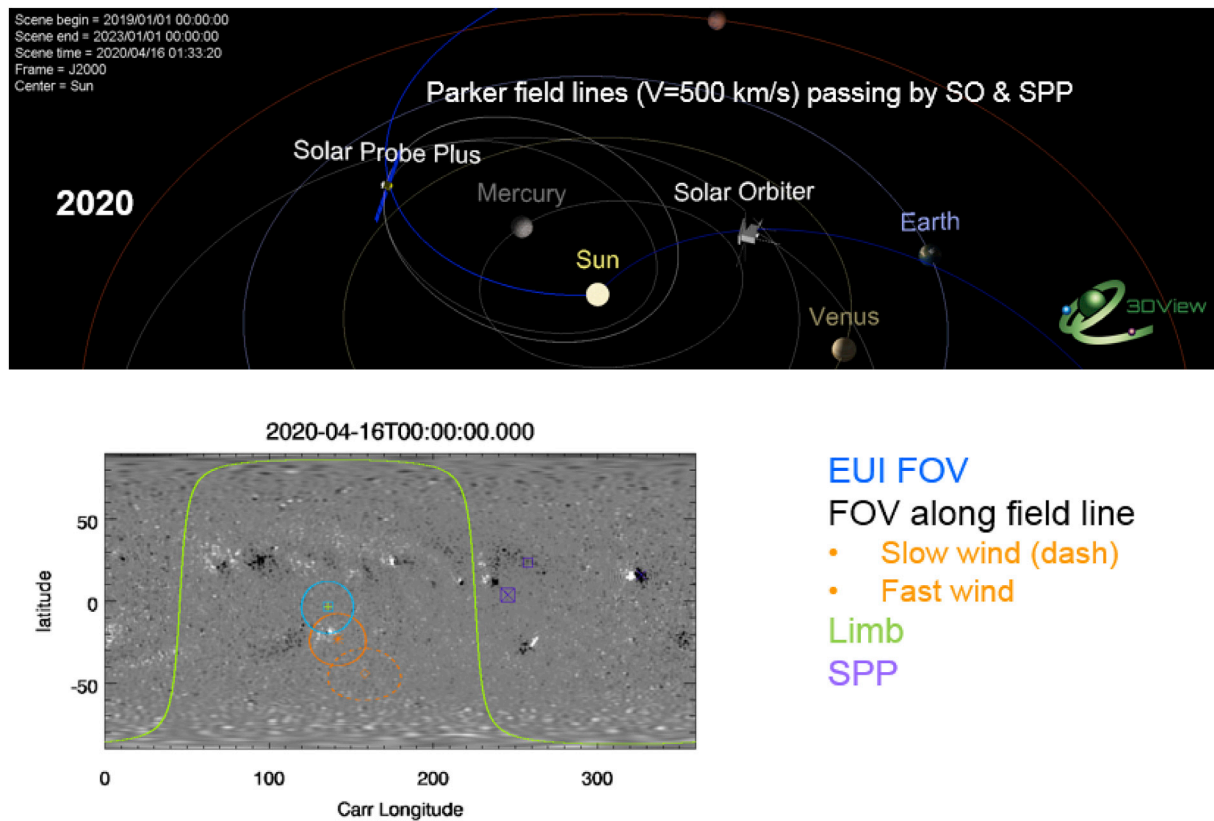


Fig. 25. A composite view of a 3DView scene (above) and ConnectSolo image (below) in the Solar Orbiter/Solar Probe Plus context (see text for details).

alternative approach is to use the capability of the ConnectSolo tool which offers systematic estimations of the connectivity between the probes and the Sun using solar wind modelling. The goal of this tool is to produce robust estimates of the paths and propagation delays of any type of disturbance (e.g. slow and fast solar wind, instantaneous particle propagation) both for post-event analysis and for connectivity forecasting. The background coronal magnetic field is currently determined via existing surface magnetograms and PFSS extrapolations, but the tool is ready to include different combinations of coronal field reconstruction methods (NLFFF, Solar Models), wind models (WSA, MVP), heliospheric models (Parker, ENLIL, EUFHORIA) and constraints from data assimilation techniques (ADAPT) as these become available. The tool will then compare the predictions made using several models in order to assess the uncertainties. The first implementation of the tool, also illustrated on the bottom of Fig. 25, uses existing magnetogram data (from years 2009–2011) transposed in time to the date of operation of Solar Orbiter and Solar Probe Plus (2019–2021, and beyond) in order to test the methods and to anticipate difficulties which may arise during the operation of the two missions. Linking 3DView and ConnectSolo is under study: on the large scale 3DView would provide 3D heliospheric representations of field lines, and zooming close to the Sun would call ConnectSolo results for display.

10. Conclusion

This paper presents the main features of a 3D space physics data visualization tool, 3DView, designed by IT engineers and scientists under the supervision of the French Plasma Physics Data Center, the CDPP. The initial “simple” orbit functionalities have been extended following 1/the involvement of CDPP in several science and interoperability EU projects, and 2/the willingness of CNES to support software for a larger community. The main focus of development in recent years has been towards the integration of a broad range of data, from in-situ measurements, to

models and numerical simulations. In this context integration means either direct upload by the user or the use of interoperability standards which facilitate the connection between tools and databases, for instance SAMP for data transfer or EPN-TAP for data discovery. Along side the community of scientists, the tool has attracted an audience among students which benefit from the 3D representations of data and get an easier understanding of some space physics concepts. Hands-on and tutorials demonstrating 3DView functionalities are regularly offered at the Masters Degree level and during summer schools. Finally, the next envisioned developments concern two aspects: first, the connection to new databases to increase the possibility of data ingestion; for instance a connection prototype to the ESA/Cluster Science Archive is in place, and the planned increase of services in the VESPA frame will naturally increase 3DView potentialities. Second, new science functionalities are currently being developed and among them a conjunction finder between space born and Earth ground based facilities. This will greatly help the ionospheric community to identify relevant case studies, access the data and display them in the same tool. “2D” functionalities will also be enhanced, in particular surface mapping, for Earth, but also at giant planets (with auroral emission data from the APIS database). In conclusion 3DView is conceived and developed as a multi-purpose, multi-thematic analysis tool which can have varied usages from precise science cases, to model exploration and mission preparation.

Acknowledgments

The CDPP wishes to warmly thank all members of its User Committee (CDPP CU) for the time spent at extensively testing functionalities and for the judicious discussions and comments. Many users, and among them numerous students, are also thanked for their useful contribution at enhancing the tool by reporting bugs, typos, ... The 3DView development team is grateful to the ViSBARD (NASA/SPDF) team for long-standing inspiration. The CDPP, and in particular the 3DView software, is

strongly supported by CNES. The “IMPEX functionalities” have been supported by the EU FP7 project “IMPEX” under grant agreement No 262863 and developed under a CNRS contract. Some functionalities were developed for the VESPA and PSWS Work-packages of the project

“Europlanet 2020 RI”. The Europlanet 2020 Research Infrastructure project has received funding from the European Union's Horizon 2020 research and innovation programme under grant agreement No 654208.

Supplementary material.

More information can be found on the CDPP and 3DView webpages. In particular a dedicated page <http://3dview.cdpp.eu/pages/supplementary.html> provides 3DView configuration files (extension .3dv) for the different science cases; these files can be loaded in the “Open file” menu of a scene to recover the context and data. This enables the interested reader to quickly replay the science cases without setting all parameters manually. Similar information for other papers and contexts are, and will be, also given on this page. Links for more video tutorials combining 3Dview and other tools can be found in [Modolo et al., 2018](#). The source code of 3DView can be found at <https://gitlab.irap.omp.eu/CDPP/3DVIEW>.

References

- Anderson, B.J., et al., 2007. The Magnetometer instrument on MESSENGER. *Space Sci. Rev.* 131, 417–450.
- André, et al., 2017. Planetary space weather services offered by the Europlanet H2020 research infrastructure. *PSS*. <http://dx.doi.org/10.1016/j.pss.2017.04.020>.
- Andrews, G.B., et al., 2007. The energetic particle and plasma spectrometer instrument on the MESSENGER spacecraft. *Space Sci. Rev.* 131, 523–556.
- Balogh, A., et al., 2001. The Cluster magnetic field investigation: overview of inflight performance and initial results. *Ann. Geophys.* 19, 1207–1217.
- Belenkaya, E.S., et al., 2013. Influence of the solar wind magnetic field on the Earth and Mercury magnetospheres in the paraboloidal model. *Planet. Space Sci.* 75.
- Cain, J.C., Ferguson, B.B., Mozzoni, D., 2003. An $n=90$ internal potential function of the Martian crustal magnetic field. *J. Geophys. Res.* 108 (E2), 5008. <http://dx.doi.org/10.1029/2000JE001487>.
- Chisham, G., Lester, M., Milan, S.E., et al., 2007. A decade of the Super Dual Auroral Radar Network (SuperDARN): scientific achievements, new techniques and future directions. *Surv. Geophys.* 28, 33. <http://dx.doi.org/10.1007/s10712-007-9017-8>.
- Dubinin, et al., 2006. Plasma morphology at Mars. Aspera-3 observations. *Space Sci. Rev.* 126, 209–238. <http://dx.doi.org/10.1007/s11214-006-9039-4>.
- Edberg, et al., 2008. Statistical analysis of the location of the Martian magnetic pileup boundary and bow shock and the influence of crustal magnetic fields. *JGR* 113, A08206. <http://dx.doi.org/10.1029/2008JA013096>.
- Erard, et al., 2014. The EPN-TAP protocol for the planetary science virtual observatory. *Astron. Comput.* 7.
- Erard, et al., 2018. VESPA: a community-driven virtual observatory in planetary science. *PSS* 150, 65–85.
- Escoubet, et al., 2001. The Cluster mission. *Ann. Geophys.* 19, 1197–1200. <http://dx.doi.org/10.5194/angeo-19-1197-2001>. <http://www.ann-geophys.net/19/1197/2001/>.
- Génot, et al., 2014. Joining the yellow hub: uses of the simple application messaging protocol in space physics analysis tools. *Astron. Comput.* 7.
- Génot, et al., 2018. TREPS, a tool for coordinate and time transformations in space physics. *PSS* 150, 86–90.
- Grasset, O., et al., 2013. JUPITER ICY moons Explorer (JUICE): an ESA mission to orbit Ganymede and to characterise the Jupiter system. *Planet. Space Sci.* 78, 1–21.
- Kallio, E., Janhunen, P., 2003. Solar wind and magnetospheric ion impact on Mercury's surface. *Geophys. Res. Lett.* 30, 1877. <http://dx.doi.org/10.1029/2003GL017842>, 17.
- Kanani, S.J., et al., 2010. A new form of Saturn's magnetopause using a dynamic pressure balance model, based on in situ, multi-instrument Cassini measurements. *J. Geophys. Res.* 115, A06207. <http://dx.doi.org/10.1029/2009JA014262>.
- Karimabadi, H., Sipes, T.B., Wang, Y., Lavraud, B., Roberts, A., 2009. A new multivariate time series data analysis technique: Automated detection of flux transfer events using Cluster data. *JGR* 114 (A6). [CiteID A06216](https://doi.org/10.1029/2009JA014262).
- Lamy, L., Prangé, R., Henry, F., Le Sidaner, P., June 2015. The auroral planetary imaging and spectroscopy (APIS) service. *Astron. Comput.* 11 (Part B), 138–145. <http://dx.doi.org/10.1016/j.ascom.2015.01.005>. ISSN 2213-1337.
- Leclercq, L., et al., 2016a. Multi-species hybrid simulations of Ganymede's magnetosphere. *PSS* submitted.
- Leclercq, L., et al., 2016b. 3D magnetospheric parallel hybrid multi-grid method applied to planet-plasma interactions. *J. Comput. Phys.* 309.
- Liu, Z.X., et al., 2005. The Double star mission. *Ann. Geophys.* 23, 2707–2712. <http://dx.doi.org/10.5194/angeo-23-2707-2005>. <http://www.ann-geophys.net/23/2707/2005/>.
- Masters, A., Achilleos, N., Dougherty, M.K., Slavin, J.A., Hospodarsky, G.B., Arridge, C.S., Coates, A.J., 2008. An empirical model of Saturn's bow shock: Cassini observations of shock location and shape. *J. Geophys. Res.* 113, A10210. <http://dx.doi.org/10.1029/2008JA013276>.
- Modolo, et al., 2016. Mars-solar wind interaction: LatHyS, an improved parallel 3-D multispecies hybrid model. *JGR Space Phys.* 121 (7).
- Modolo, et al., 2018. The LatHyS database for planetary plasma environment investigations. Comparison between MAVEN, Mars Express and simulation results - a case study. *PSS* 150, 13–21.
- Moldovan, et al., 2011. Mercury's magnetopause and bow shock from MESSENGER observations. *EPSC Abstr.* 6. EPSC-DPS2011-674, EPSC-DPS Joint Meeting 2011.
- Parker, E.N., 1958. Dynamics of the interplanetary gas and magnetic fields. *Astrophys. J.* 128, 664.
- Pei, C., Bieber, J.W., Burger, R.A., Clem, J., 2012. Three-dimensional wavy heliospheric current sheet drifts. *Astrophys. J.* 744 <http://dx.doi.org/10.1088/0004-637X/744/2/170>, 170 (5pp).
- Pitout, F., Dunlop, M.W., Blagau, A., Bogdanova, Y.V., Escoubet, C.P., Carr, C., Dandouras, I., Fazakerley, A.N., 2008. Coordinated Cluster and Double Star observations of the dayside magnetosheath and magnetopause at different latitudes near noon. *J. Geophys. Res.* <http://dx.doi.org/10.1029/2007JA012767>.
- Plotnikov, I., Rouillard, A.P., Davies, J.A., Bothmer, V., Eastwood, J.P., Gallagher, P., Harrison, R.A., Kilpua, E., Möstl, C., Perry, C.H., Rodriguez, L., Lavraud, B., Génot, V., Pinto, R.F., Sanchez-Diaz, E., 2016. Long-term tracking of corotating density structures using heliospheric imaging. *Sol. Phys.* 291 (6).
- Richer, E., Modolo, R., Chanteur, G.M., Hess, S., Leblanc, F., 2012. A global hybrid model for Mercury's interaction with the solar wind: case study of the dipole representation. *J. Geophys. Res. Space Phys.* 117, A10.
- Rouillard, et al., 2008. First imaging of corotating interaction regions using the STEREO spacecraft. *GRL* 35 (10).
- Rouillard, et al., 2017. A propagation tool to connect remote-sensing observations with in-situ measurements of heliospheric structures. *PSS* arXiv:1702.00399.
- Shue, J.-H., Chao, J.K., Fu, H.C., Russell, C.T., Song, P., Khurana, K.K., Singer, H.J., 1997. A new functional form to study the solar wind control of the magnetopause size and shape. *J. Geophys. Res.* 102 (A5), 9497–9512.
- Sibeck, D.G., Lopez, R.E., Roelof, E.C., 1991. Solar wind control of the magnetopause shape, location, and motion. *J. Geophys. Res.* 96, 5489–5495.
- Slavin, J.A., et al., 1985. Solar wind flow about the outer planets: gasdynamic modelling of the Jupiter and Saturn bow shocks. *JGR* 90 (A7), 6275–6286. <http://dx.doi.org/10.1029/JA090iA07p06275>.
- Slavin, et al., 2009. MESSENGER observations of Mercury's magnetosphere during northward IMF. *GRL* 36, L02101. <http://dx.doi.org/10.1029/2008GL036158>.
- Smirnov, et al., 1980. An empirical model of the Venusian outer environment 2. The shape and location of the bow shock. *JGR* 85 (A3), 7651–7654. <http://dx.doi.org/10.1029/JA085iA13p07651>.
- ESA/SRE Solar Orbiter Definition Study Report, 2011, p. 14.
- Solomon, S.C., McNutt Jr., R.L., Gold, R.E., Domingue, D.L., 2007. MESSENGER mission overview. *Space Sci. Rev.* 131, 3–39.
- Taylor, M.B., 2005. TOPCAT & STIL: starlink table/VOTable processing software, astronomical data analysis software and systems XIV ASP Conference series. In: Shopbell, P., Britton, M., Ebert, R. (Eds.), *Proceedings of the Conference Held 24-27 October, 2004 in Pasadena, California, USA*, vol. 347. Astronomical Society of the Pacific, San Francisco, p. 29.
- Troignon, et al., 2006. Martian shock and magnetic pile-up boundary positions and shapes determined from the Phobos 2 and Mars Global Surveyor data sets. *Planet. Space Sci.* 54, 357–369. <http://dx.doi.org/10.1016/j.pss.2006.01.003>.
- Tsyganenko, N.A., 1995. Modeling the Earth's magnetospheric magnetic field confined within a realistic magnetopause. *J. Geophys. Res.* 100, 5599–5612.
- Winslow, R.M., Anderson, B.J., Johnson, C.L., Slavin, J.A., Korth, H., Purucker, M.E., Baker, D.N., Solomon, S.C., 2013. Mercury's magnetopause and bow shock from MESSENGER Magnetometer observations. *J. Geophys. Res. Space Phys.* 118, 2213–2227. <http://dx.doi.org/10.1002/jgra.50237>.
- Witasse, et al., 2017. Interplanetary coronal mass ejection observed at STEREO-A, Mars, comet 67P/Churyumov-Gerasimenko, Saturn, and New Horizons en-route to Pluto. Comparison of its Forbush decreases at 1.4, 3.1 and 9.9 AU, *JGR*. <http://dx.doi.org/10.1002/2017JA023884>.

Web References¹

CDPP. <http://www.cdpp.eu>

¹ The references are listed according to the order in which each resource occurs in the paper.

3DView. <http://3dview.cdpp.eu>
IMPEX. <http://impex-fp7.oeaw.ac.at>
TREPS. <http://treps.cdpp.eu>
Java3D. <https://java3d.java.net>
AMDA. <http://amda.cdpp.eu>
SSCWeb. <http://sscweb.gsfc.nasa.gov/>
SAMP. <http://www.ivoa.net/documents/SAMP/>
VOTable. <http://www.ivoa.net/documents/VOTable/>
CLWeb. <http://clweb.irap.omp.eu>
CDAWeb. <http://cdaweb.gsfc.nasa.gov>
CCMC. <http://ccmc.gsfc.nasa.gov>
VESPA. <http://euoplanet-vespa.eu/>

IPDA. <http://planetarydata.org/>
SPASE. <http://www.spase-group.org/>
Gitlab for the JAVA EPN-TAP library. <https://gitlab.irap.omp.eu/OV-GSO-DC/EpriTAPClient>
High resolution map of Ganymede. http://photojournal.jpl.nasa.gov/jpegMod/PIA12564_modest.jpg
APIS. <http://apis.obspm.fr/>
HELcats. <https://www.helcats-fp7.eu/>
LatHyS. <http://impex.latos.ipsl.fr/LatHyS.htm>
ALADIN. <http://aladin.u-strasbg.fr/>
ConnectSolo. <http://storms-connectsolo.irap.omp.eu>